Journal of the Franklin Institute 362 (2025) 108253

Contents lists available at ScienceDirect

Journal of the Franklin Institute

journal homepage: www.elsevier.com/locate/fi

Fuzzy control for input-saturated stochastic high-order nonlinear systems: A dual flexible performance-preset boundary-based approach

Ziyi Liu [a], Yangang Yao [a,*], Yu Kang [b,*], Yunbo Zhao [b], Jieqing Tan [c], Lichuan Gu [a,*], Qiang Li [a]

[a] School of Information and Artificial Intelligence, Anhui Agricultural University, Hefei, 230036, China
[b] Department of Automation, University of Science and Technology of China, Hefei, 230027, China
[c] School of Mathematics, Hefei University of Technology, Hefei, 230601, China

ARTICLE INFO

Keywords:
Input saturation
Stochastic high-order nonlinear systems
Dual flexible performance- preset boundary
Fuzzy control

ABSTRACT

This article presents a dual flexible performance-preset boundary (DFPPB)-based fuzzy control approach for input-saturated stochastic high-order nonlinear systems. Distinct from most of the existing prescribed performance control approaches, the initial PPB of which remains bounded and fixed, meaning that they can only suit for nonlinear systems where the initial error information is completely known. By designing a rate function-based PPB, the proposed algorithm can be used in many cases where the initial error information is completely known, partially known and completely unknown without changing the control structure. In addition, by designing an auxiliary system and embedding its output into PPB, and a novel DFPPB and a tensile model-based barrier function are constructed, so that the proposed algorithm achieves autonomous coordination between performance preset and input security. Furthermore, the unknown nonlinear functions are approached by the fuzzy logic systems, and the results show that the designed DFPPB-based fuzzy control algorithm guarantees that all closed-loop signals remain semi-globally bounded in probability; the system output is capable of effectively tracking the desired signal, while the tracking error is consistently kept within the DFPPB. The developed algorithm is illustrated by means of simulation instances.

1. Introduction

It is well known that stochastic disturbances are unavoidable in real systems, so the control of stochastic systems has garnered considerable attention, and many innovative control algorithms were proposed, see [1–5] and their references. Note that earlier algorithms mainly focused on general stochastic feedback nonlinear systems, as a class of stochastic systems with more general structure and non-feedback linearization, stochastic high-order nonlinear systems (SHONSs) can describe the dynamic characteristics of complex systems more accurately, and the control of SHONSs has become a research focus in the control field. Just name a list, an output tracking control of SHONSs with application to benchmark mechanical system was presented in [6]. An adaptive state-feedback stabilization of SHONSs with stochastic inverse dynamics and time-varying powers was proposed in [7]. Min et al. [8]

* Corresponding authors.
E-mail addresses: 24721982@stu.ahau.edu.cn (Z. Liu), ygyao@ustc.edu.cn (Y. Yao), kangduyu@ustc.edu.cn (Y. Kang), ybzhao@ustc.edu.cn (Y. Zhao), jqt20202020@126.com (J. Tan), glc@ahau.edu.cn (L. Gu), nunliqiang@126.com (Q. Li).

https://doi.org/10.1016/j.jfranklin.2025.108253
Received 13 August 2025; Received in revised form 13 October 2025; Accepted 13 November 2025
Available online 17 November 2025
0016-0032/

presented an adaptive stabilization of SHONSs subject to uncertainties. Two control approaches of SHONSs with output constraints were obtained in [9,10]. Yao et al. [11] presented a unified fuzzy control approach for SHONSs with or without state constraints. It should be pointed out that the transient/steady-state control performance is less considered in the above methods.

With the improvement of users' requirements, the transient/steady state control performance of the actual system becomes increasingly important. For steady-state performance, many finite, fixed, and prescribed-time stability control (Hereinafter referred to as "finite-time control (FTC)") algorithms were proposed [12–18]. The prescribed performance control (PPC) first obtained in [19] is an effective method to achieve superior transient control performance, and be widely used in the control design of many kinds of systems [20–24]. The core of the above PPC methods (called "traditional PPC (TPPC)") is to design an exponential-type PPB so that the tracking error be always enveloped within the PPB. In order to take into account both tracking accuracy and convergence time, many approaches that combine FTC and PPC were proposed [25–28]. The shortcoming of this fusion is that it increases the complexity of control design to some extent. To address this challenge, Zhao et al. [29] designed a finite-time PPC (FTPPC) algorithm by constructing a novel finite-time PPB (FTPPB), which enabling both convergence time and tracking accuracy to be preset. This approach has since been extended to nonlinear systems with diverse structures [30–34], thereby broadening its applicability. Nonetheless, an inherent limitation exists in both the FTPPC and TPPC methods is that the initial PPB remains bounded and fixed. This implies that when the initial state or reference signal changes, the users have to double check whether the initial PPB can envelope the new initial error, and if not, the new PPB needs to be selected again. What is more serious is that the above method is only applicable to the case where the initial error information is completely known, and for some specific control systems, the initial error information may be partially known, or even completely unknown, then the above methods become useless. Then, the delayed PPC (DPPC) methods were proposed to map the initial PPB to infinite boundary by mapping transformation [35–37], which effectively enrich the PPC theory when the initial error information is completely unknown. Of course, the limitation of DPPC methods is also obvious, i.e., whether the initial error information is known, partially unknown or completely unknown, its initial PPB must always be infinite, when the error information is known or partially unknown, it will inevitably lead to the decline of the initial transient performance. Then, a unified PPC (UPPC) approach was proposed [38], which can adapt to many cases where the initial error is completely known, partially known and completely unknown. Recently, the UPPC method was extended to SISO systems [39–41] and MIMO systems [42]. It is noted that the above methods do not consider the influence of performance preset on the control signal, and assume that the control signal can be infinite. Meanwhile, the above methods are limited to general feedback systems or deterministic HONSs, which are difficult to apply to IS-SHONSs.

Limited by the device load and other factors, the control input of actual control system must have a maximum allowable range. If the control signal exceeds the maximum allowable threshold, the device may be damaged and security risks may arise. As a result, the existing literatures have presented a lot of PPC approaches for input-saturated nonlinear systems (ISNSs). For instance, two TPPC approaches for ISNSs were presented in [43,44], under which an auxiliary system is constructed to dispose the input saturation. Shen et al. [45] presented a FTPPC approach of input-saturated 2-DOF helicopter. The above approaches to address input saturation share a same goal, i.e., to transform saturated input into manageable normal input through various transformations. Unfortunately, all of the above methods deal with input saturation and performance preset in isolation, while ignoring the coupling effect between them, which makes the above PPC methods extremely "fragile". For example, when the performance preset is severe, the control signal will increase to exceed the allowable threshold, replacing the control signal with the threshold will cause the error to increase, and even exceed the PPB, resulting in singularity. To this end, some fragility-free flexible PPC (FPPC) approaches were presented recently. For instance, Yong et al. [46] first established a novel PPB related to input saturation, and the coordination between input security and performance preset is realized. The idea was recently extended to ISNSs with different forms [47–53]. The aforementioned methods, however, are also only suitable for ISNSs where the initial error information is completely known, and most of them are limited to general feedback systems, but cannot be directly applied to input-saturated SHONSs (IS-SHONSs) where the initial error is partially known and completely unknown.

Based on the above analysis, this article dedicates to propose a DFPPB-based fuzzy control approach for IS-SHONSs, which can not only be used in many cases where the initial error information is completely known, partially known and completely unknown without changing the control structure, but also can realize the autonomous coordination between input safety and performance preset. The main innovations are summarized below

1) This article first presents a DFPPB-based fuzzy control approach for IS-SHONSs. Distinct from the TPPC approaches [19–24], the FTPPC approaches [29–34] for nonlinear systems without considering the input saturation, and the FPPC approaches of ISNSs [46–52], the initial PPB of which remains bounded and fixed, meaning that the above approaches can only suit for nonlinear systems where the initial error information is completely known. Furthermore, when the initial state or reference signal changes, the users have to double check whether the initial PPB can envelope the new initial error, and if not, the new PPB needs to be selected again. By designing a rate function (RF)-based PPB, the proposed algorithm can be used in many cases where the initial error information is completely known, partially known and completely unknown without changing the control structure, thereby significantly enhancing the flexibility and application scope of the algorithm.
2) Unlike the UPPC approaches [38–42], the TPPC approaches [43,44], and FTPPC approach [45], they either ignore the input saturation or deal with performance preset and input saturation in isolation, which leads to the hidden trouble of input security or the difficulty of coordination between performance presets and input security. By designing an auxiliary system and embedding its output into PPB, and a novel DFPPB and a tensile model-based barrier function are constructed, so that the proposed algorithm achieves autonomous coordination between performance preset and input security (see Remark 3 for details). In addition, the unknown nonlinear functions are approached by the fuzzy logic systems (FLSs). The results show that the designed DFPPB-based

fuzzy control algorithm guarantees that all closed-loop signals remain semi-globally bounded in probability (SGBIP); the system output is capable of effectively tracking the desired signal, while the tracking error is consistently kept within the DFPPB.

2. Problem statement and preliminaries

2.1. Problem formulation

Give an IS-SHONS as follows

$$\begin{cases} \mathrm{d}x_i = \left(f_i\left(\bar{\boldsymbol{x}}_i\right) + x_{i+1}^{p_i}\right)\mathrm{d}t + \hbar_i^{\mathrm{T}}\left(\bar{\boldsymbol{x}}_i\right)\mathrm{d}w, \\ \mathrm{d}x_n = \left(f_n\left(\bar{\boldsymbol{x}}_n\right) + \mathrm{S}^{p_n}(v)\right)\mathrm{d}t + \hbar_n^{\mathrm{T}}\left(\bar{\boldsymbol{x}}_n\right)\mathrm{d}w, \\ y = x_1 \end{cases} \tag{1}$$

where $i = 1, 2, \cdots, n-1$, $\bar{\boldsymbol{x}}_i = \left[x_1, \cdots, x_i\right]^{\mathrm{T}}$ represents the system state vector, v is the designed controller, y represents the system output, $\mathrm{S}(v)$ represents the system input. $\hbar_i(\cdot)$ and $f_i(\cdot)$ represent the function vector and uncertain nonlinear function. $w \in \mathbf{R}^r$ denotes an independent standard Brownian motion, $p_i \in \mathbf{R}_{odd}^{\geq 1} = \left\{p \geq 1 \middle| p = q_1/q_2\right\}$, $q_j \in \boldsymbol{R}^+(j = 1, 2)$ with $i = 1, 2, \cdots, n$, and

$$\mathrm{S}(v) = \begin{cases} v, & |v| \leq \bar{v} \\ \mathrm{sign}(v)\bar{v}, & |v| > \bar{v} \end{cases} \tag{2}$$

where $\bar{v}$ is the maximum permissible threshold of the control input.

Utilize the following estimation to deal with the acute angles of $\mathrm{S}(v)$

$$\mathrm{S}(v) = k_1(v) + k_2(v) \tag{3}$$

with $k_1(v) = \bar{v}\tanh(v/\bar{v})$, $k_2(v) = \mathrm{S}(v) - k_1(v)$, and $|k_2(v)| \leq \bar{v}(1 - \tanh(1)) = \bar{k}$.

On the basis of the Mean Value Theorem, for $\forall v_0 \in \boldsymbol{R}$, we can obtain

$$k_1'\left(v_1\right) = \frac{k_1(v) - k_1\left(v_0\right)}{v - v_0} \tag{4}$$

where $v_1 = v_0 + \lambda\left(v - v_0\right)$ with $\lambda \in (0, 1)$. Let $k_0 = k_1'\left(v_1\right)$, from the expression of $k_1(v)$ it follows that $0 < \underline{k} \leq k_0^{p_n} < 1$, where $\underline{k}$ is an unknown constant. By setting $v_0 = 0$, (3) can be rewritten as

$$\mathrm{S}(v) = k_0 v + k_2(v). \tag{5}$$

Then, one can further gain

$$\mathrm{S}^{p_n}(v) = k_0^{p_n} v^{p_n} + K(v) \tag{6}$$

where $K(v) = \left(k_0 v + k_2(v)\right)^{p_n} - \left(k_0 v\right)^{p_n}$. Since $K(v) \to 0$ when $v \to \infty$, it follows that $K(v)$ is bounded. Therefore, $\exists \bar{K} > 0$, such that $K(v) \leq \bar{K}$.

This article aims to construct a novel DFPPB-based fuzzy control algorithm guarantees that all closed-loop signals remain SGBIP; the system output is capable of effectively tracking the desired signal, while the tracking error is always kept within the DFPPB.

2.2. Preliminaries

Definition 1. For the following stochastic system

$$\mathrm{d}x = f(x)\mathrm{d}t + \hbar(x)\mathrm{d}w, \tag{7}$$

$V(x)$ is a $\boldsymbol{C}^2$ positive-definite function, the differential operator $\mathscr{L}$ of $V(x)$ is as follows

$$\mathscr{L}V(x) = \frac{\partial V(x)}{\partial x} f(x) + \frac{1}{2}\mathrm{Tr}\left(\hbar^{\mathrm{T}}(x)\frac{\partial^2 V(x)}{\partial x^2}\hbar(x)\right) \tag{8}$$

where $\mathrm{Tr}(\cdot)$ represents the trace of $\cdot$.

Lemma 1. *[8]: For system (7), assume that there exists a $\boldsymbol{C}^2$ Lyapunov function (LF) $V(\boldsymbol{x})$: $\boldsymbol{R}^n \to \boldsymbol{R}^+$, functions $\aleph_1(\cdot), \aleph_2(\cdot) \in \boldsymbol{\mathcal{K}}_\infty$, $c, d \in \boldsymbol{R}^+$, such that*

$$\begin{cases} \aleph_1(||\boldsymbol{x}||) \leq V(\boldsymbol{x}) \leq \aleph_2(||\boldsymbol{x}||), \\ \mathscr{L}V(\boldsymbol{x}) \leq -cV(\boldsymbol{x}) + d \end{cases}$$

then the system almost surely has a unique solution, all the closed-loop signals remain SGBIP, and satisfying

$$\mathbb{E}(V) \leq V(\mathbf{0})\exp(-ct) + \frac{d}{c} \tag{9}$$

where $\mathbb{E}(\cdot)$ represents the expectation of $\cdot$.

Lemma 2. *[8]:A FLS can approximate the unknown nonlinear function $\bar{f}(\mathcal{X})$ as follows:*

$$\bar{f}(\mathcal{X}) = \boldsymbol{\Upsilon}^{\mathrm{T}}\boldsymbol{\Psi}(\mathcal{X}) + \epsilon(\mathcal{X}), \quad \left(|\epsilon(\mathcal{X})| \le \epsilon, \epsilon \in \boldsymbol{R}^{+}\right) \tag{10}$$

where $\mathcal{X}, \boldsymbol{\Upsilon}, \boldsymbol{\Psi}(\mathcal{X}), \epsilon(\mathcal{X})$ represents input, weight, the basis function, and error of the FLS, respectively. $\boldsymbol{\Psi}(\mathcal{X}) = \left[\Psi_1(\mathcal{X}), \cdots, \Psi_m(\mathcal{X})\right]^{\mathrm{T}} / \sum_{i=1}^{m} \Psi_i(\mathcal{X})$, $m > 1$ stands for the number of the fuzzy rules. Choose $\Psi_i(\mathcal{X})$ as $\Psi_i(\mathcal{X}) = \exp\left(-\left(\mathcal{X} - \boldsymbol{\iota}_i\right)^{\mathrm{T}}\left(\mathcal{X} - \boldsymbol{\iota}_i\right)/\varsigma_i{}^2\right), i = 1, \cdots, m$ with ς_i and $\boldsymbol{\iota}_i$ represent the center vector and the spreads of $\Psi_i(\mathcal{X})$.

Lemma 3. *[9]: For $r \in \boldsymbol{R}_{odd}^{\ge 1}$, $x, y \in \boldsymbol{R}$, $\iota, \jmath, \gamma, a \in \boldsymbol{R}^{+}$, one has*

$$|x^r - y^r| \le r(2^{r-2} + 2)|x - y|\left(|x - y|^{r-1} + y^{r-1}\right), \tag{11}$$

$$a|x|^{\iota}|y|^{\jmath} \le \frac{\gamma\iota}{\iota + \jmath}|x|^{\iota+\jmath} + \frac{\jmath a^{\frac{\iota+\jmath}{\jmath}}}{\iota + \jmath}\gamma^{-\frac{\iota}{\jmath}}|y|^{\iota+\jmath}. \tag{12}$$

Lemma 4. *[9]: For $\iota \ge 0, \jmath > 0$ and $\gamma \ge 1$, we have*

$$\iota \le \jmath + \left(\frac{\iota}{\gamma}\right)^{\gamma}\left(\frac{\gamma - 1}{\jmath}\right)^{\gamma-1}. \tag{13}$$

3. Main results

3.1. Dual flexible performance preset boundary (DFPPB)

Design a RF-based PPB as follows

$$\mathscr{H}(\Gamma(t)) = \frac{\ell\Gamma(t)}{\sqrt{1 - \Gamma^2(t)}} \tag{14}$$

where $\Gamma(t) = \left(\Gamma_0 - \Gamma_{\mathrm{T}}\right)\zeta(t) + \Gamma_{\mathrm{T}}$, $\ell, \Gamma_{\mathrm{T}}, \Gamma_0$ satisfying $0 < \Gamma_{\mathrm{T}} < \Gamma_0 \le 1$, $\ell > 0$. $\zeta(t)$ represents the RF, possesses the following characteristics: (1)$\zeta(0) = 1$ and $\zeta(t) \in [0, 1), \forall t > 0$; (2)$\zeta^{(i)}(t)$ is piece-wise continuous and bounded with $i = 0, \cdots, n$. Here, $\zeta(t)$ is chosen as follows

$$\zeta(t) = \begin{cases} \left(\frac{\mathrm{T}-t}{\mathrm{T}}\right)^{n+1}, & 0 \le t < \mathrm{T} \\ 0, & t \ge \mathrm{T} \end{cases} \tag{15}$$

where T and n stand for the design constant and the order of the system, respectively.

A tensile model-based barrier function is designed as follows

$$s = \frac{\beta(t)}{\left(\vartheta_1 + \beta(t)\right)\left(\vartheta_2 - \beta(t)\right)} \tag{16}$$

where $\vartheta_1, \vartheta_2 \in (0, 1], \beta(t) = \eta(t)/\Gamma(t)$, $\eta(t) = M(\sigma)e_1/\sqrt{M^2(\sigma)e_1^2 + \ell^2}$ with $e_1 = x_1 - y_r$, y_r denotes the desired signal. $M(\sigma) = \exp(-\tau\sigma)$ represents the tensile function with $\tau \in \boldsymbol{R}^{+}$, and σ denotes the output of the following auxiliary system

$$\dot{\sigma} = -\rho_1\sigma + \rho_2\left(b_1(t) + b_2(t)\right), \sigma(0) = 0 \tag{17}$$

where $\rho_1, \rho_2 \in \boldsymbol{R}^{+}$, $b_1(t) = (\operatorname{sign} \upsilon - \bar{\upsilon} + 1)(\upsilon - \bar{\upsilon})$, $b_2(t) = (\operatorname{sign} \upsilon + \bar{\upsilon} - 1)(\upsilon + \bar{\upsilon})$.

Remark 1. Analysis of the expressions of $b_1(t)$ and $b_2(t)$ reveals that $b_1(t) + b_2(t) \equiv 0$ if and only if $|\upsilon| \le \bar{\upsilon}$, conversely, when $|\upsilon| > \bar{\upsilon}$, it holds that $b_1(t) + b_2(t) > 0$. Additionally, from (17), it can be inferred that $\sigma = 0$ when $|\upsilon| \le \bar{\upsilon}$, whereas $\sigma > 0$ when $|\upsilon| > \bar{\upsilon}$. Given the formulation of $M(\cdot)$, it follows that $M(\sigma) \in (0, 1]$, and $M(\sigma) = 1$ if and only if $|\upsilon| \le \bar{\upsilon}$.

The DFPPB is expressed as $\left(\underline{\mathcal{G}}(t), \bar{\mathcal{G}}(t)\right)$ with

$$\begin{cases} \underline{\mathcal{G}}(t) = \frac{\mathscr{H}\left(-\vartheta_1\Gamma(t)\right)}{M(\sigma)}, \\ \bar{\mathcal{G}}(t) = \frac{\mathscr{H}\left(\vartheta_2\Gamma(t)\right)}{M(\sigma)} \end{cases} \tag{18}$$

where

$$\begin{cases} \mathscr{H}\left(-\vartheta_1\Gamma(t)\right) = \frac{-\ell\vartheta_1\Gamma(t)}{\sqrt{1-\left(\vartheta_1\Gamma(t)\right)^2}}, \\ \mathscr{H}\left(\vartheta_2\Gamma(t)\right) = \frac{\ell\vartheta_2\Gamma(t)}{\sqrt{1-\left(\vartheta_2\Gamma(t)\right)^2}}. \end{cases} \tag{19}$$

From (16), it can be deduced that when $\beta(0) \in \left(-\vartheta_1, \vartheta_2\right)$ holds with bounded s, then $\beta(t) \in \left(-\vartheta_1, \vartheta_2\right)$ holds for $\forall t \in \boldsymbol{R}^{+}$. Further analysis of the expression of $\beta(t)$ reveals that $\beta(t) \in \left(-\vartheta_1, \vartheta_2\right)$ is equivalent to $\eta(t) \in \left(-\vartheta_1\Gamma(t), \vartheta_2\Gamma(t)\right)$. Given that (14) establishes $\mathscr{H}(\cdot)$ as a strictly monotonically increasing function of $\cdot$, then $\eta(t) \in \left(-\vartheta_1\Gamma(t), \vartheta_2\Gamma(t)\right)$ is further equivalent to

$$\mathscr{H}\left(-\vartheta_1\Gamma(t)\right) < \mathscr{H}(\eta(t)) < \mathscr{H}\left(\vartheta_2\Gamma(t)\right). \tag{20}$$

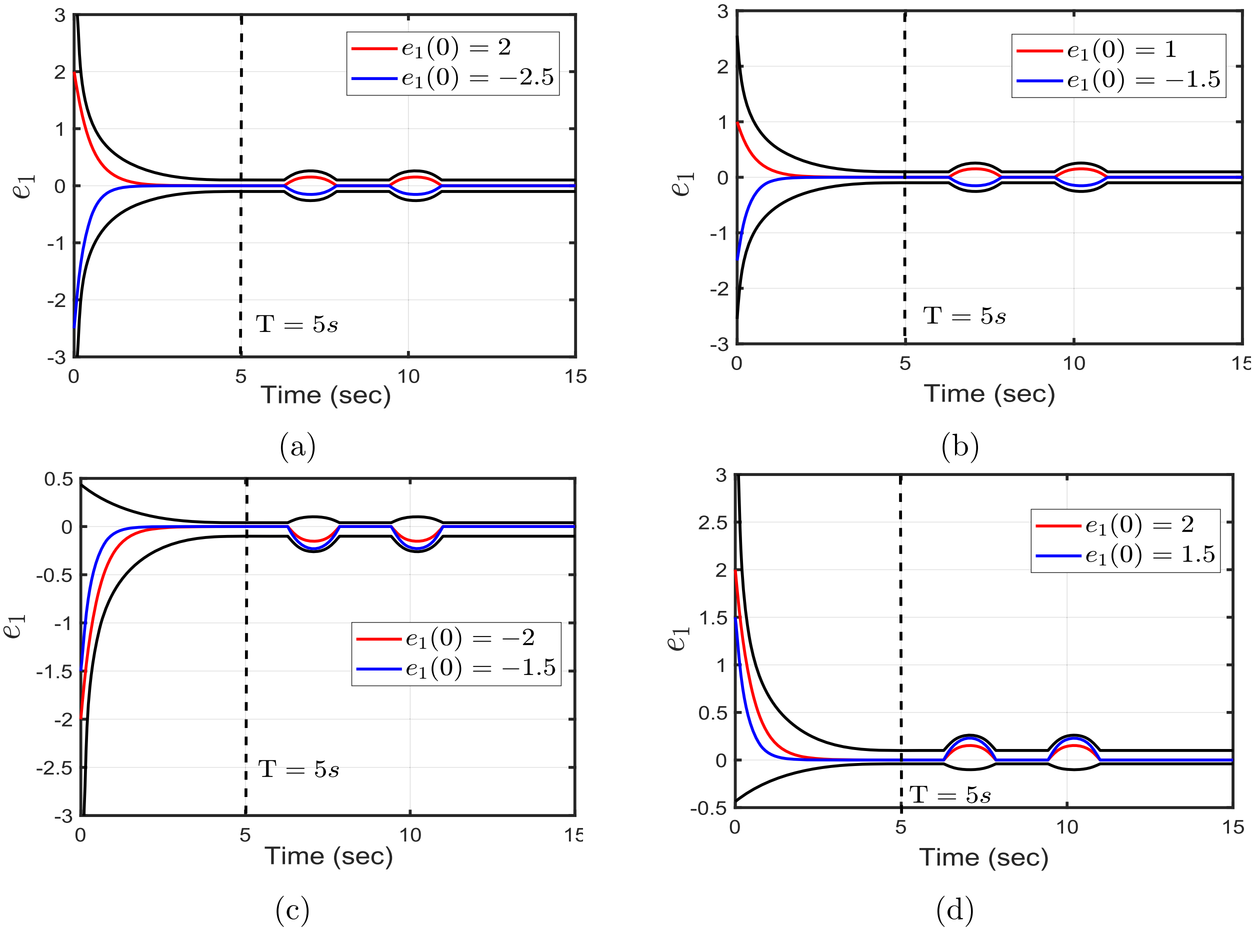

Fig. 1. Diagram of the corresponding DFPPB under different parameters: (a) $\vartheta_1 = \vartheta_2 = \Gamma_0 = 1$;(b) $0 < \vartheta_1, \vartheta_2, \Gamma_0 < 1$; (c) $\vartheta_2 = \Gamma_0 = 1, 0 < \vartheta_1 < 1$; (d) $\vartheta_1 = \Gamma_0 = 1, 0 < \vartheta_2 < 1$.

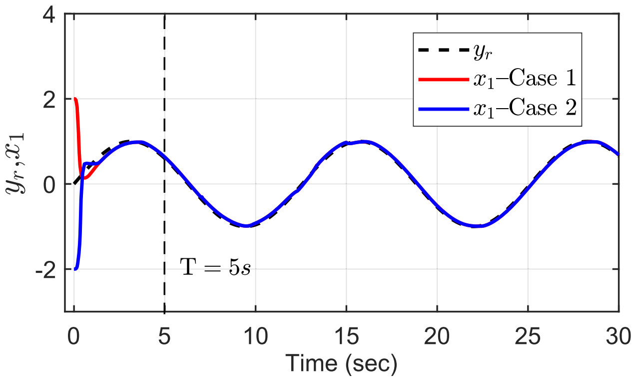

Fig. 2. The tracking curves under two different cases.

From (20), one obtains

$$\mathscr{H}\left(-\vartheta_1\Gamma(t)\right) < M(\sigma)e_1 < \mathscr{H}\left(\vartheta_2\Gamma(t)\right). \tag{21}$$

The above analysis demonstrates that if $e_1(0) \in \left(\underline{\mathcal{G}}(0), \bar{\mathcal{G}}(0)\right) = \left(\mathscr{H}\left(-\vartheta_1\Gamma(0)\right), \mathscr{H}\left(\vartheta_2\Gamma(0)\right)\right)$ and s remains bounded, $e_1(t) \in \left(\underline{\mathcal{G}}(t), \bar{\mathcal{G}}(t)\right)$ holds for $\forall t \in \boldsymbol{R}^+$. This indicates that introducing the barrier function (16) effectively converts the performance constraint control into the bounded control for s.

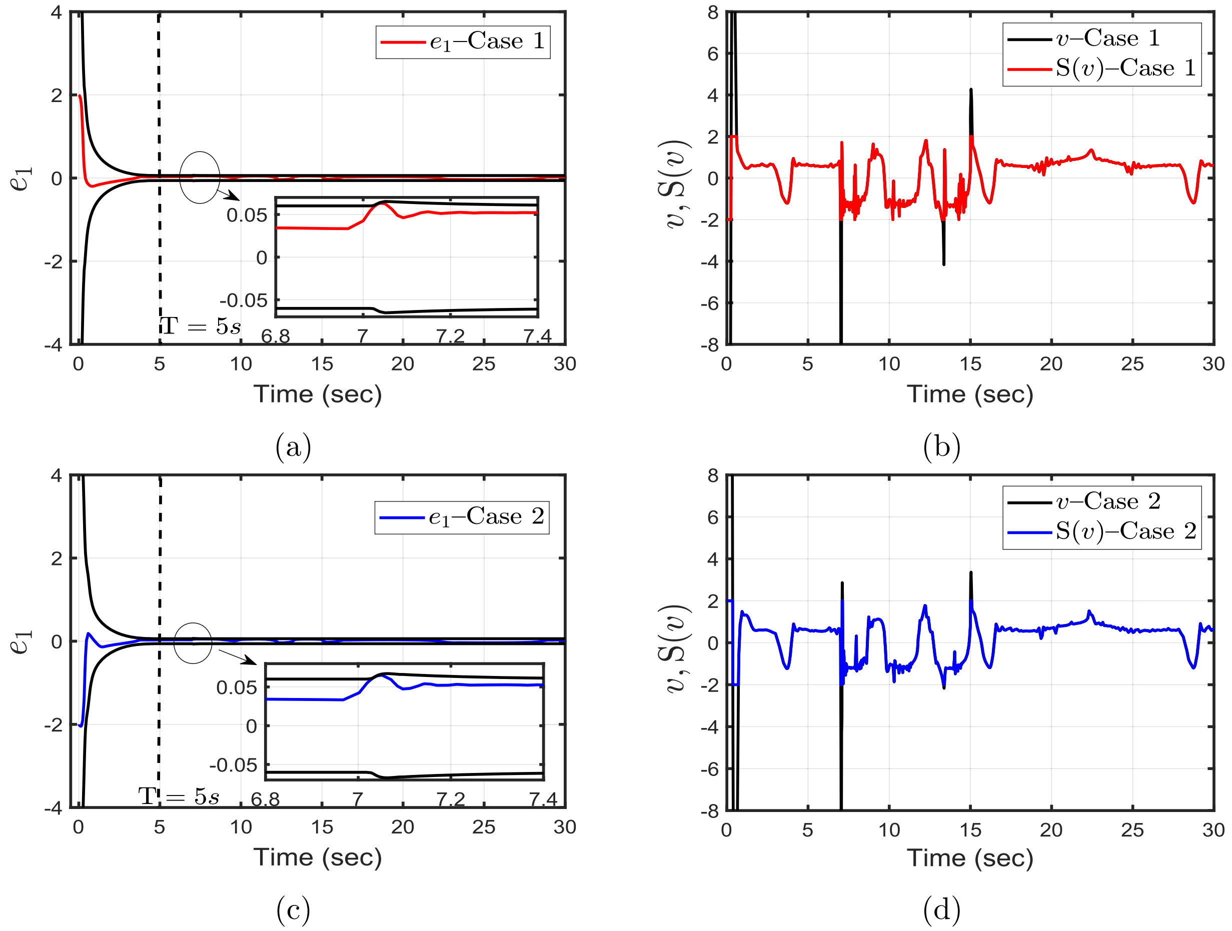

Fig. 3. (a)(b) respectively represents the tracking curve and control input curve in case 1;(c)(d) respectively represents the tracking curve and control input curve in case 2.

Remark 2. Distinct from the TPPC approaches [19–24], the FTPPC approaches [29–34] for nonlinear systems without considering the input saturation (i.e., $M(\sigma) \equiv 1$), and the FPPC approaches of ISNSs [46–52], the initial PPB of which remains bounded and fixed, meaning that the above approaches can only suit for nonlinear systems where the initial error information is completely known. Nevertheless, the proposed algorithm can be used in many cases where the initial error information is completely known, partially known and completely unknown without changing the control structure.

- Let $\vartheta_1 = \vartheta_2 = \Gamma_0 = 1$, it follows from (18) and (19) that $\underline{\mathcal{G}}(0) \to -\infty$ and $\bar{\mathcal{G}}(0) \to +\infty$, i.e., $e_1(0) \in (-\infty, +\infty)$. It indicates that the proposed algorithm is suit for the scenario where the initial error is entirely unknown, as illustrated in Subgraph (a) of Fig. 1;
- Let $\vartheta_1, \vartheta_2, \Gamma_0 \in (0,1)$, it follows from (18) and (19) that $\underline{\mathcal{G}}(0) = \mathscr{H}\left(-\vartheta_1\Gamma(0)\right) = \underline{\mathcal{G}}$ and $\bar{\mathcal{G}}(0) = \mathscr{H}\left(\vartheta_2\Gamma(0)\right) = \bar{\mathcal{G}}$ ($\underline{\mathcal{G}} < 0$ and $\bar{\mathcal{G}} > 0$ denote the bounded constants), i.e., $e_1(0) \in \left(\underline{\mathcal{G}}, \bar{\mathcal{G}}\right)$. It indicates that the proposed algorithm is applicable for the scenario where the initial error is entirely known, as illustrated in Subgraph (b) of Fig. 1. In fact, in this scenario, the proposed approach reduces to the conventional FTPPC approach [29,30];
- Let $\vartheta_2 = \Gamma_0 = 1, \vartheta_1 \in (0,1)$, it follows from (18) and (19) that $\underline{\mathcal{G}}(0) = \mathscr{H}\left(-\vartheta_1\Gamma(0)\right) = \underline{\mathcal{G}} < 0$ ($\underline{\mathcal{G}}$ denotes a bounded constant) and $\bar{\mathcal{G}}(0) \to +\infty$, i.e., $e_1(0) \in \left(\underline{\mathcal{G}}, +\infty\right)$. It indicates that the proposed method is applicable for any scenario with $\operatorname{sign} e_1(0) = 1$, as illustrated in Subgraph (c) of Fig. 1;
- Let $\vartheta_1 = \Gamma_0 = 1, 0 < \vartheta_2 < 1$, it follows from (18) and (19) that $\bar{\mathcal{G}}(0) = \mathscr{H}\left(\vartheta_2\Gamma(0)\right) = \bar{\mathcal{G}} > 0$ ($\bar{\mathcal{G}}$ denote a bounded constant) and $\underline{\mathcal{G}}(0) \to -\infty$, i.e., $e_1(0) \in \left(-\infty, \bar{\mathcal{G}}\right)$. It indicates that the proposed method is applicable for any scenario with $\operatorname{sign} e_1(0) = -1$, as illustrated in Subgraph (d) of Fig. 1.

Remark 3. Unlike the UPPC approaches [38–42], the TPPC approaches [43,44], and FTPPC approach [45], they either ignore the input saturation or deal with performance preset and input saturation in isolation, which leads to the hidden trouble of input security or the difficulty of coordination between performance preset and input security. In this article, by designing the auxiliary system (17) and embedding its output into PPB, and the novel DFPPB (18) and the tensile model-based barrier function (16) are constructed.

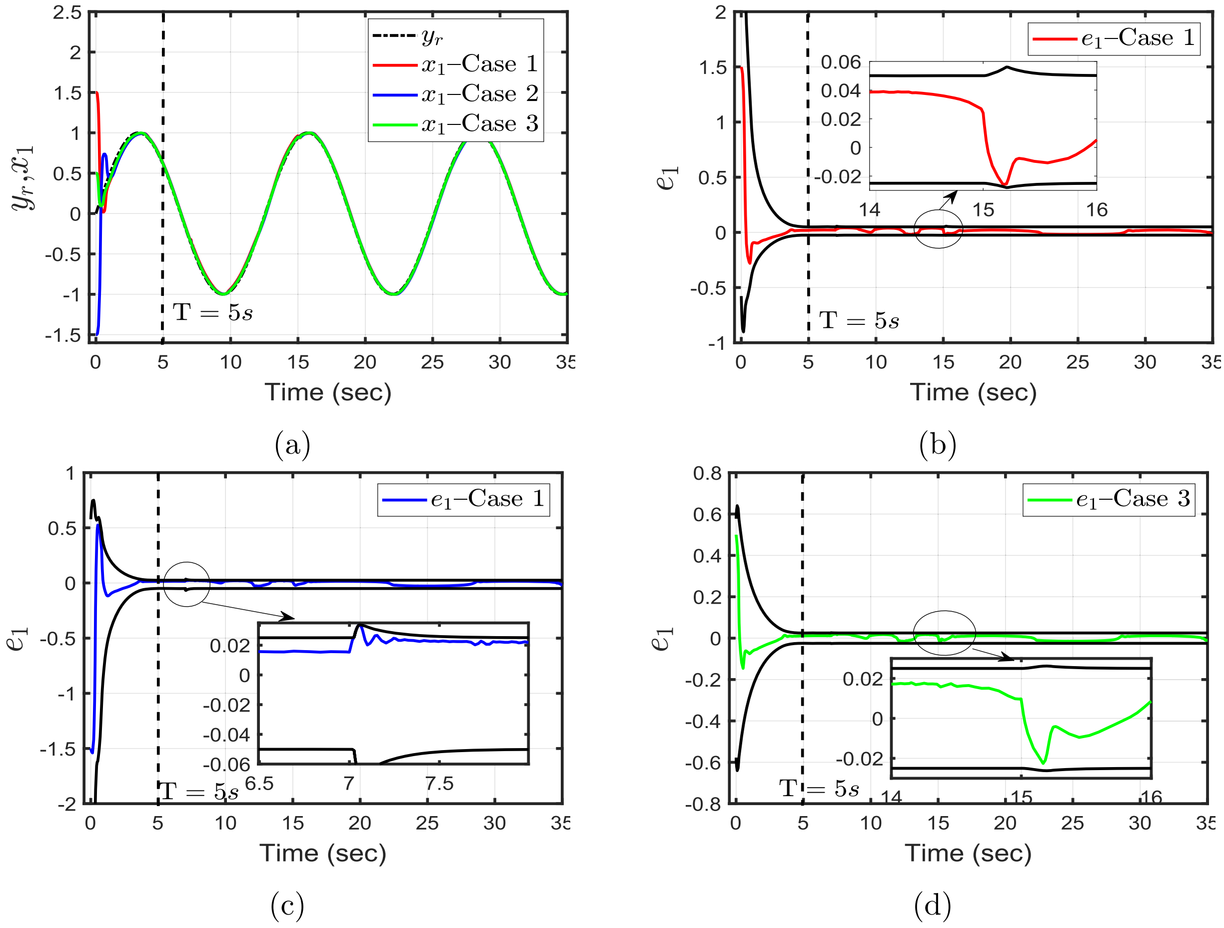

Fig. 4. (a) represent the tracking curves in three cases;(b)(c)(d) respectively represent the tracking curves under three cases.

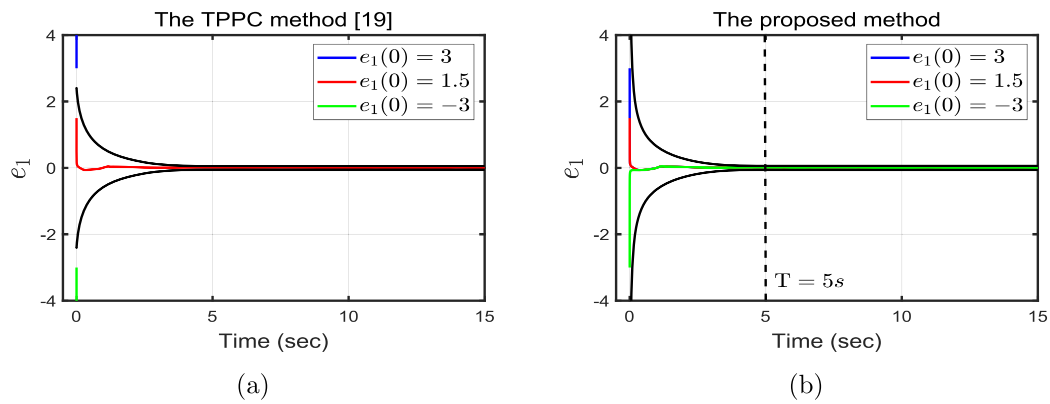

Fig. 5. (a)(b) represent the tracking error curves under the action of TPPC method [19] and the proposed method under three cases, respectively.

According to (17) and Remark 1, one know that the tensile function $M(\sigma) \in (0, 1]$, and $M(\sigma) = 1$ if and only if $|v| \leq \bar{v}$. In combination with (18), one can further obtain that when $|v| > \bar{v}$ (i.e., the control signal exceeds its maximum allowable threshold), the DFPPB will adapt to expand to avoid singularity, and when$|v| \leq \bar{v}$, the DFPPB will automatically revert to the original PPB, so that the proposed algorithm achieves autonomous coordination between performance preset and input security. The schematic diagram is shown in Subgraphs (a)-(d) in Fig. 1.

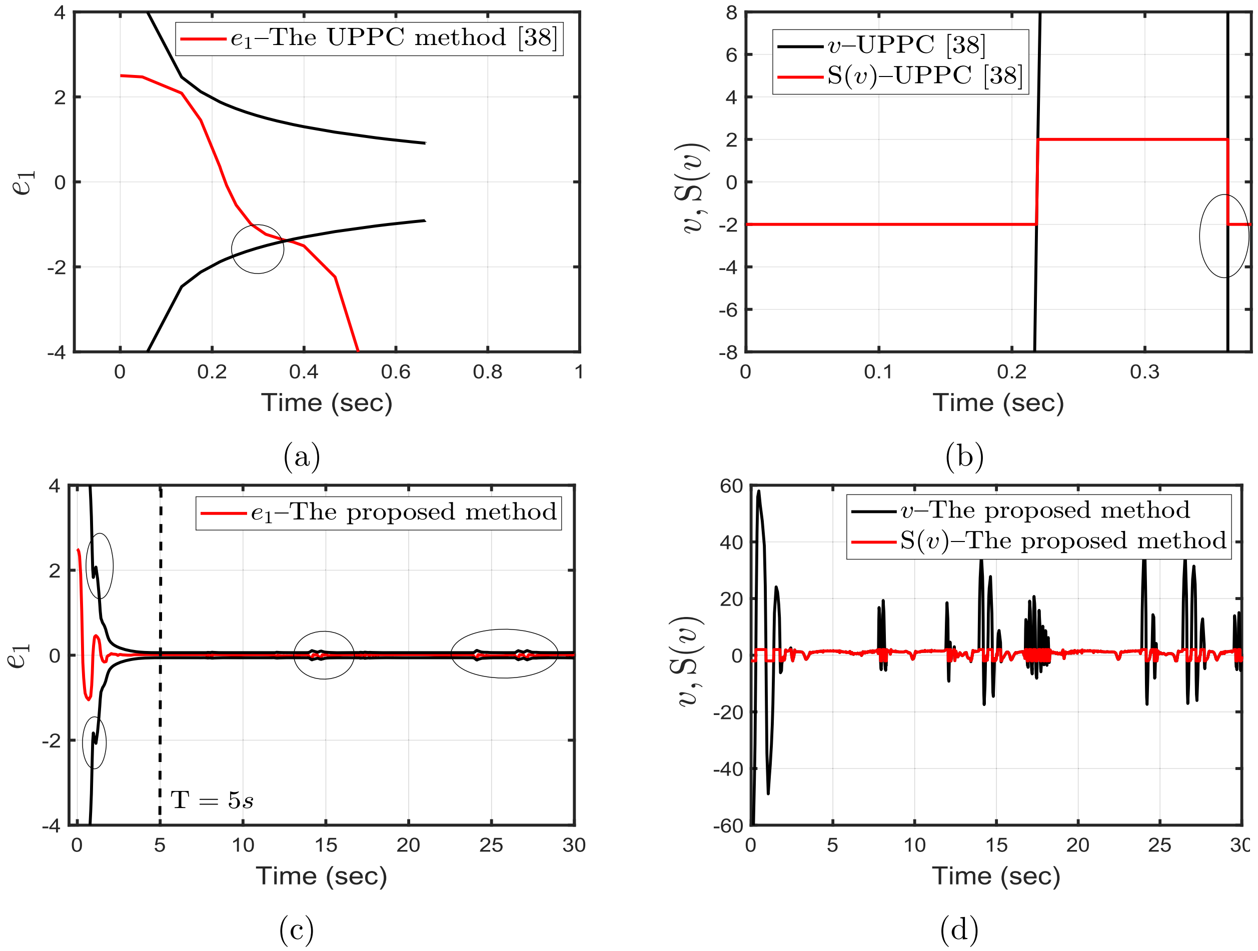

Fig. 6. (a)(b) respectively represent the tracking error curve and control input curve under the action of the UPPC method [38]; (c)(d) respectively represent the tracking error curve and control input curve under the action of the proposed method.

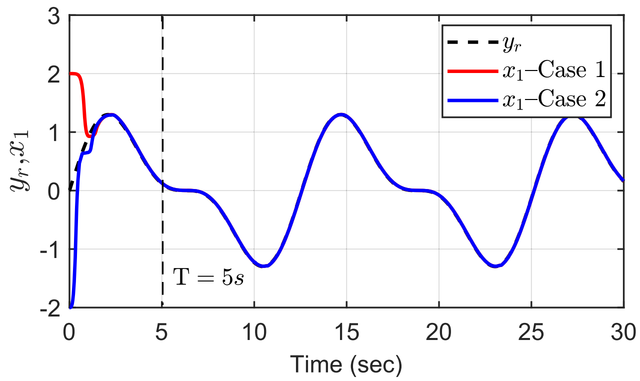

Fig. 7. The tracking curves under two different cases.

3.2. DFPPB-Based Fuzzy controller design

From (16), we obtain

$$\mathrm{d}s = \mu_1 \mathrm{d}e_1 + \mu_2 \mathrm{d}t \tag{22}$$

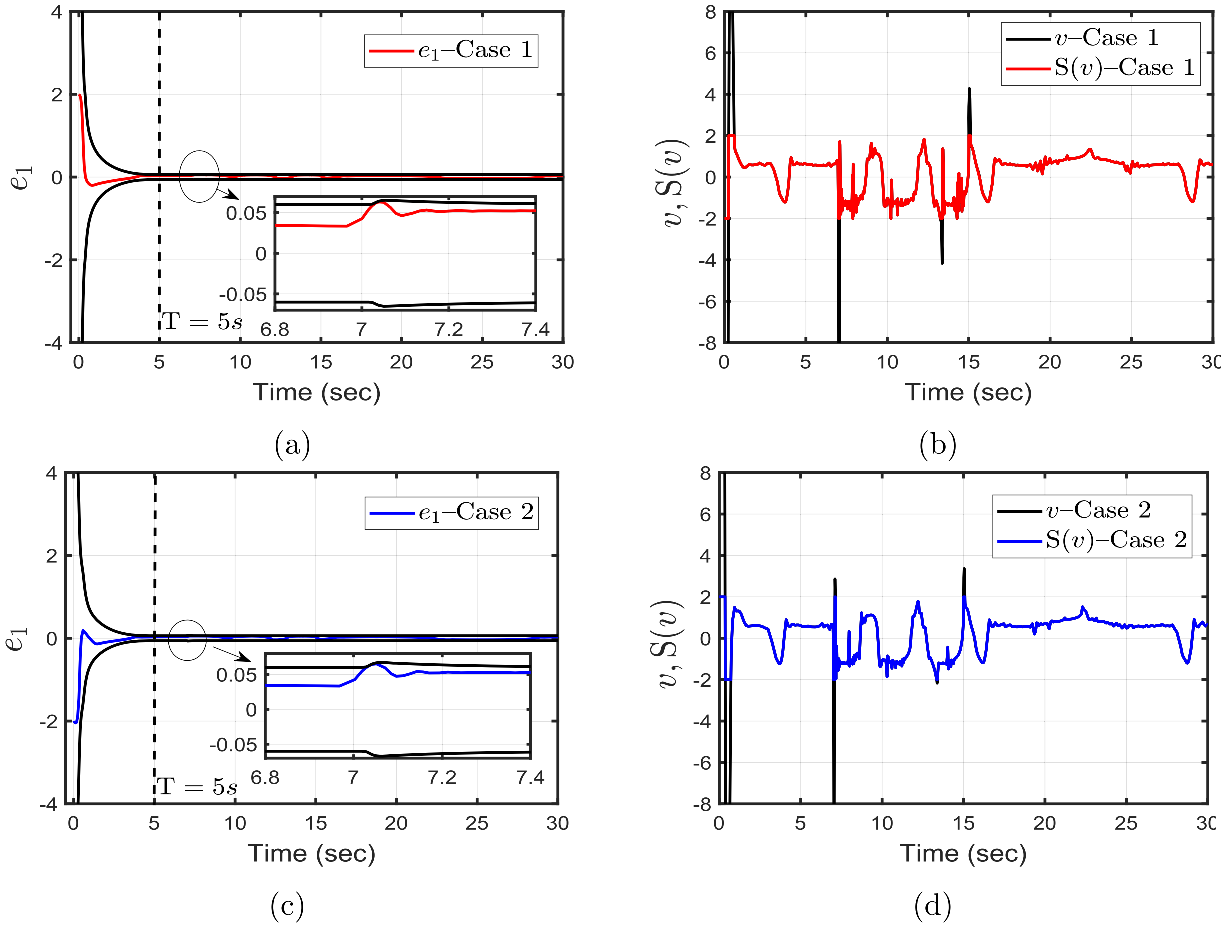

Fig. 8. (a)(b) respectively represents the tracking curve and control input curve in case 1;(c)(d) respectively represents the tracking curve and control input curve in case 2.

where

$$\mu_2 = \left(\left(\vartheta_1\vartheta_2+\beta^2\right)e_1\left(\dot{M}-\eta M e_1 \dot{M}-\dot{\Gamma}\eta\right)\right)\Big/\left(\Gamma^2\left(\vartheta_1+\beta\right)^2\left(\vartheta_2-\beta\right)^2\sqrt{M^2e_1^2+\ell^2}\right),$$
$$\mu_1 = \left(\left(\vartheta_1\vartheta_2+\beta^2\right)M\ell^2\right)\Big/\left(\Gamma\left(\vartheta_1+\beta\right)^2\left(\vartheta_2-\beta\right)^2\left(M^2e_1^2+\ell^2\right)\sqrt{M^2e_1^2+\ell^2}\right)$$

with $\beta=\beta(t)$, $M=M(\sigma(t))$, $\eta=\eta(t)$, $\Gamma=\Gamma(t)$.

Let $\varrho_1=s, \varrho_i=x_i-\alpha_{i-1}, i=2,\cdots,n$. From (1) and (22), one obtains

$$\begin{cases} \mathrm{d}\varrho_1=\mu_1\left(F_1(x_1)+x_2^{p_1}\right)\mathrm{d}t+\boldsymbol{H}_1^{\mathrm{T}}dw, \\ \mathrm{d}\varrho_i=\left(F_i(\bar{\boldsymbol{x}}_i)+x_{i+1}^{p_i}\right)\mathrm{d}t+\boldsymbol{H}_i^{\mathrm{T}}dw, \\ \mathrm{d}\varrho_n=\left(F_n(\bar{\boldsymbol{x}}_n)+\mathrm{S}^{p_n}(v)\right)\mathrm{d}t+\boldsymbol{H}_n^{\mathrm{T}}dw \end{cases} \tag{23}$$

where $F_1(x_1)=f_1(x_1)-\dot{y}_d+\mu_2/\mu_1$, $F_i(\bar{\boldsymbol{x}}_i)=f_i(\bar{\boldsymbol{x}}_i)-\mathscr{L}\alpha_{i-1}$ with $i=2,\cdots,n$, $\boldsymbol{H}_1^{\mathrm{T}}=\mu_1\hbar_1^{\mathrm{T}}(x_1)$, $\boldsymbol{H}_i=\hbar_i(\bar{\boldsymbol{x}}_i)-\sum_{j=1}^{i-1}(\partial\alpha_{i-1}/x_j)\hbar_j(\bar{\boldsymbol{x}}_j)$, α_i represents the virtual control signal. Let $\Theta_i=||\boldsymbol{\Upsilon}_i||^2, i=1,2,\cdots,n$, $\boldsymbol{\Upsilon}_i$ represents the weight vector of FLS, $\tilde{\Theta}_i=\Theta_i-\hat{\Theta}_i$, $\hat{\Theta}_i$ represents the estimate of Θ_i, $p=\max_{1\le i\le n}\{p_i\}$, $P_i=p-p_i+4$.

Step 1: Introduce the LF V_1 as

$$V_1=\frac{1}{P_1}\varrho_1^{P_1}+\frac{1}{2r_1}\tilde{\Theta}_1^2, \quad (r_1\in\boldsymbol{R}^+). \tag{24}$$

From (23)-(24), we obtain

$$\mathscr{L}V_1=\varrho_1^{P_1-1}\mu_1\left(F_1(x_1)+x_2^{p_1}\right)+\frac{P_1-1}{2}\varrho_1^{P_1-2}\|\boldsymbol{H}_1\|^2-\frac{1}{r_1}\tilde{\Theta}_1\dot{\hat{\Theta}}_1. \tag{25}$$

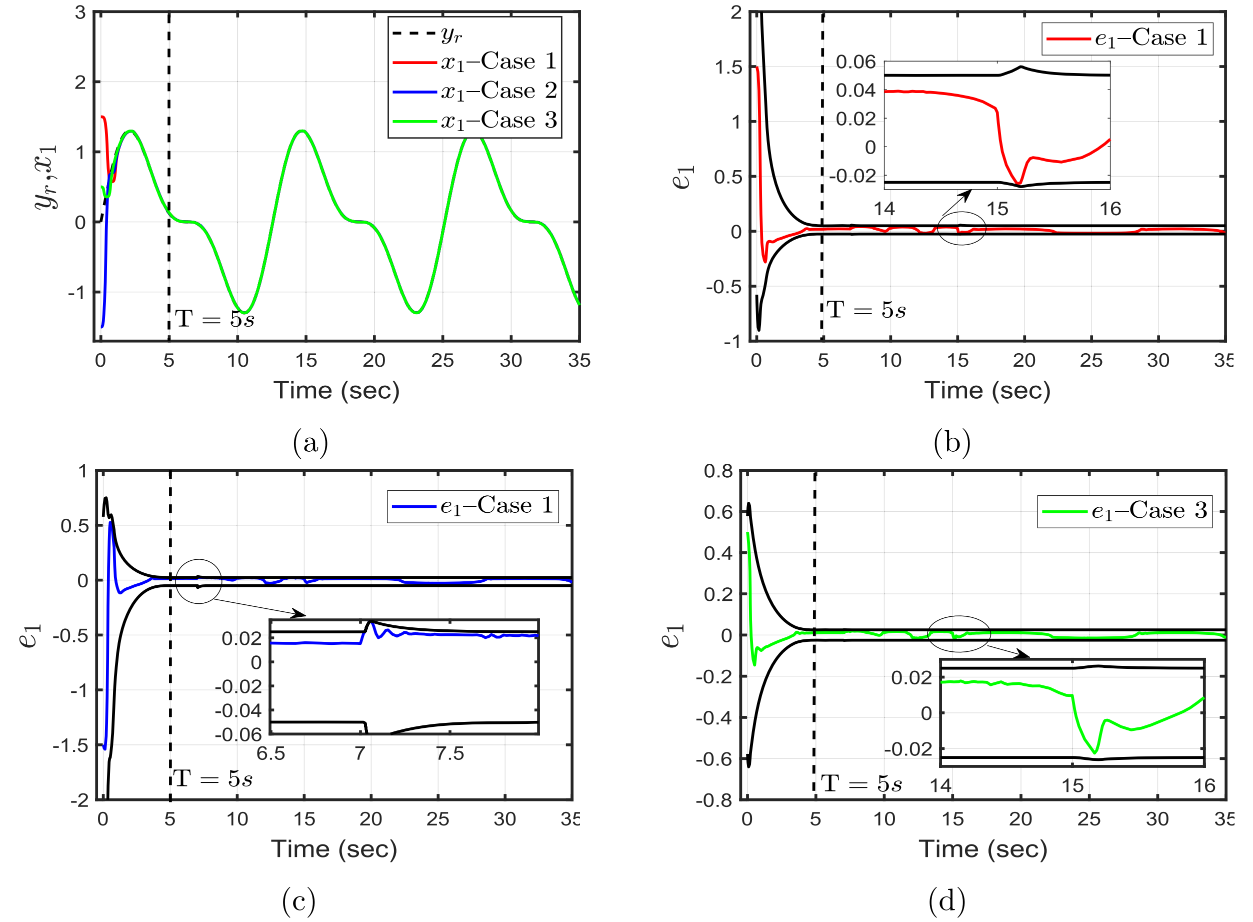

Fig. 9. (a) represent the tracking curves under three cases; (b)(c)(d) respectively represent the tracking curves under three cases.

From (12), one obtains

$$\varrho_1^{P_1-2}\|\boldsymbol{H}_1\|^2 \le \frac{1}{2}\varrho_1^{2P_1-4}\|\boldsymbol{H}_1\|^4 + \frac{1}{2}. \tag{26}$$

Substituting (26) into (25), one obtains

$$\begin{aligned}\mathscr{L}V_1 \le& \mu_1\varrho_1^{P_1-1}(x_2^{p_1}-\alpha_1^{p_1}) + \mu_1\varrho_1^{P_1-1}\alpha_1^{p_1} + \varrho_1^{P_1-1}\bar{f}_1(\boldsymbol{\mathcal{X}}_1)\\ &+ \frac{P_1-1}{4} - \frac{\tilde{\Theta}_1\dot{\hat{\Theta}}_1}{r_1} - \frac{P_1-1}{P_1}\varrho_1^{P_1} - \mu_1\Xi_1\varrho_1^{p+3}\end{aligned} \tag{27}$$

where $\bar{f}_1(\boldsymbol{\mathcal{X}}_1) = \mu_1 F_1(x_1) + (P_1-1)\varrho_1^{P_1-3}\|\boldsymbol{H}_1\|^4/4 + (P_1-1)\varrho_1/P_1 + \mu_1\Xi_1\varrho_1^{p_1}$ with $\boldsymbol{\mathcal{X}}_1 = [x_1, y_r]^{\mathrm{T}}$, Ξ_1 will be derived in the subsequent analysis.

It follows Lemma 2 that $\bar{f}_i(\boldsymbol{\mathcal{X}}_i)$ can be effectively approximated via a FLS, i.e., $\bar{f}_i(\boldsymbol{\mathcal{X}}_i) = \epsilon_i(\boldsymbol{\mathcal{X}}_i) + \boldsymbol{\Upsilon}_i^{\mathrm{T}}\boldsymbol{\Psi}_i(\boldsymbol{\mathcal{X}}_i)$, where $|\epsilon_i(\boldsymbol{\mathcal{X}}_i)| \le \epsilon_i$ with $\epsilon_i \in \boldsymbol{R}^+$.

Given that Lemma 2–3, we obtain

$$\varrho_1^{P_1-1}\bar{f}_1(\boldsymbol{\mathcal{X}}_1) \le \frac{|\varrho_1|^{P_1-1}\tilde{\Theta}_1||\boldsymbol{\Psi}_1(\boldsymbol{\mathcal{X}}_1)||^2}{4a_1} + \varrho_1^{p+3}\Phi_1 + \frac{P_1-1}{P_1}\varrho_1^{P_1} + \frac{\epsilon_1^{P_1}}{P_1} + \varepsilon_1, \tag{28}$$

$$\varrho_1^{P_1-1}(x_2^{p_1}-\alpha_1^{p_1}) \le \frac{p_1+1}{p+3}\varrho_2^{p+3} + \Xi_1\varrho_1^{p+3} \tag{29}$$

where $a_1, \varepsilon_1 \in \boldsymbol{R}^+$, and $\Phi_1 = [(P_1-1)\psi_1/(p+3)]^{(p+3)/(P_1-1)}[p_1/(P_1-1)\varepsilon_1]^{p_1/(P_1-1)}$, $\psi_1 = \sqrt{1+\hat{\Theta}_1^2}||\boldsymbol{\Psi}_1(\boldsymbol{\mathcal{X}}_1)||^2/4a_1 + a_1$, $\Xi_1 = \left((P_1-1)\xi_1^{(p+3)/(P_1-1)} + (p+2)(\xi_1|\Omega_1|^{p_1-1})^{(p+3)/(p+2)}\right)/(p+3)$, $\xi_1 = p_1(2^{p_1-2}+2)$, Ω_1 will be given later.

Design α_1 and $\dot{\hat{\Theta}}_1$ as

$$\alpha_1 \triangleq -\Omega_1\varrho_1, \tag{30}$$

$$\Omega_1 = \left[\frac{1}{\mu_1}\left(\frac{\mathscr{B}_1}{P_1}c_1 + \Phi_1\right)\right]^{\frac{1}{p_1}}, \tag{31}$$

$$\dot{\hat{\Theta}}_1 = \frac{r_1|\varrho_1|^{P_1-1}||\boldsymbol{\Psi}_1(\boldsymbol{\mathcal{X}}_1)||^2}{4a_1} - \gamma_1\hat{\Theta}_1, \left(\hat{\Theta}_1(0) > 0\right) \tag{32}$$

where $c_1, \gamma_1 \in \boldsymbol{R}^+$, and $\mathscr{B}_1 = P_1/(p+3)$.

Substituting (28)-(32) to (27), one obtains

$$\mathscr{L}V_1 \le -\frac{c_1\mathscr{B}_1}{P_1}\varrho_1^{p+3} + \frac{\gamma_1}{r_1}\tilde{\Theta}_1\hat{\Theta}_1 + \frac{p_1+1}{p+3}\mu_1\varrho_2^{p+3} + d_1 \tag{33}$$

where $d_1 = \varepsilon_1 + \epsilon_1^{P_1}/P_1 + (P_1-1)/4$.

Step i ($i = 2, \cdots, n-1$): Introduce the LF V_i as

$$V_i = V_{i-1} + \frac{1}{P_i}\varrho_i^{P_i} + \frac{1}{2r_i}\tilde{\Theta}_i^2, \quad (r_i \in \boldsymbol{R}^+). \tag{34}$$

From (34), we obtain

$$\mathscr{L}V_i = -\sum_{j=1}^{i-1}\left(\frac{c_j\mathscr{B}_j}{P_j}\varrho_j^{p+3} - \frac{\gamma_j\tilde{\Theta}_j\hat{\Theta}_j}{r_j} - d_j\right) + \varrho_i^{P_i-1}\bar{f}_i(\boldsymbol{\mathcal{X}}_i) + \varrho_i^{P_i-1}\left(x_{i+1}^{p_i} - \alpha_i^{p_i}\right)$$
$$+ \varrho_i^{P_i-1}\alpha_i^{p_i} - \Xi_i\varrho_i^{p+3} - \frac{P_i-1}{P_i}\varrho_i^{P_i} + \frac{P_i-1}{4} - \frac{1}{r_i}\tilde{\Theta}_i\dot{\hat{\Theta}}_i \tag{35}$$

where $\bar{f}_2(\boldsymbol{\mathcal{X}}_2) = F_2(\bar{\boldsymbol{x}}_2) + [(p_1+1)\mu_1\varrho_2^{p_2}]/(p+3) + \Xi_2\varrho_2^{p_2} + (P_2-1)\varrho_2/P_2 + (P_2-1)\varrho_2^{P_2-3}\|\boldsymbol{H}_2\|^4/4$, $\bar{f}_i(\boldsymbol{\mathcal{X}}_i) = F_i(\bar{\boldsymbol{x}}_i) + [(p_{i-1}+1)\varrho_i^{p_i}]/(p+3) + \Xi_i\varrho_i^{p_i} + (P_i-1)\varrho_i/P_i + (P_i-1)\varrho_i^{P_i-3}\|\boldsymbol{H}_i\|^4/4$ with $i = 3, \cdots, n-1$, $\boldsymbol{\mathcal{X}}_i = [\bar{\boldsymbol{x}}_i, y_r]^{\mathrm{T}}$ with $i = 2, \cdots, n-1$, Ξ_i will be derived in the subsequent analysis.

Given that Lemma 2–3, one obtains

$$\varrho_i^{P_i-1}\bar{f}_i(\boldsymbol{\mathcal{X}}_i) \le \frac{|\varrho_i|^{P_i-1}\tilde{\Theta}_i||\boldsymbol{\Psi}_i(\boldsymbol{\mathcal{X}}_i)||^2}{4a_i} + \varrho_i^{p+3}\Phi_i + \frac{P_i-1}{P_i}\varrho_i^{P_i} + \frac{\Delta_i^{P_i}}{P_i} + \varepsilon_i, \tag{36}$$

$$\varrho_i^{P_i-1}\left(x_{i+1}^{p_i} - \alpha_i^{p_i}\right) \le \frac{p_i+1}{p+3}\varrho_{i+1}^{p+3} + \Xi_i\varrho_i^{p+3} \tag{37}$$

where $\varepsilon_i, a_i \in \boldsymbol{R}^+$, and $\Phi_i = [((P_i-1)\psi_i)/(p+3)]^{(p+3)/(P_i-1)}[p_i/(P_i-1)\varepsilon_i]^{p_i/(P_i-1)}$, $\psi_i = \sqrt{1+\hat{\Theta}_i^2}||\boldsymbol{\Psi}_i(\boldsymbol{\mathcal{X}}_i)||^2/4a_i + a_i$, $\Xi_i = \left((p+2)(\xi_i|\Omega_i|^{p_i-1})^{(p+3)/(p+2)} + (P_i-1)\xi_i^{(p+3)/(P_i-1)}\right)/(p+3)$, $\xi_i = p_i(2^{p_i-2}+2)$, Ω_i will be given later.

Design α_i and $\dot{\hat{\Theta}}_i$ as

$$\alpha_i \triangleq -\Omega_i\varrho_i, \tag{38}$$

$$\Omega_i = \left(\frac{\mathscr{B}_i}{P_i}c_i + \Phi_i\right)^{\frac{1}{p_i}} \tag{39}$$

$$\dot{\hat{\Theta}}_i = \frac{r_i|\varrho_n|^{P_i-1}||\boldsymbol{\Psi}_i(\boldsymbol{\mathcal{X}}_i)||^2}{4a_i} - \gamma_i\hat{\Theta}_i, \left(\hat{\Theta}_i(0) > 0\right), \tag{40}$$

where $c_i, \gamma_i \in \boldsymbol{R}^+$ and $\mathscr{B}_i = P_i/(p+3)$.

Substituting (36)-(40) to (35), one obtains

$$\mathscr{L}V_i \le -\sum_{j=1}^{i}\left(\frac{c_j\mathscr{B}_j}{P_j}\varrho_j^{p+3} - \frac{\gamma_j}{r_j}\tilde{\Theta}_j\hat{\Theta}_j - d_j\right) + \frac{p_i+1}{p+3}\varrho_{i+1}^{p+3} \tag{41}$$

where $d_j = \varepsilon_j + \epsilon_j^{P_j}/P_j + (P_j-1)/4$.

Step n: Introduce the LFc V_n as

$$V_n = V_{n-1} + \frac{1}{P_n}\varrho_n^{P_n} + \frac{1}{2r_n}\tilde{\Theta}_n^2, \quad (r_n \in \boldsymbol{R}^+). \tag{42}$$

From (6) and (42), we obtain

$$\mathscr{L}V_n \le -\sum_{j=1}^{n-1}\left(\frac{c_j\mathscr{B}_j}{P_j}\varrho_j^{p+3} - \frac{\gamma_j\tilde{\Theta}_j\hat{\Theta}_j}{r_j} - d_j\right) + \varrho_n^{P_n-1}\left(F_n(\bar{\boldsymbol{x}}_n) + k_0^{p_n}v^{p_n} + K(v)\right)$$
$$+ \frac{p_{n-1}+1}{p+3}\varrho_n^{p+3} + \frac{P_n-1}{2}\varrho_n^{P_n-2}\|\boldsymbol{H}_n\|^2 - \frac{1}{r_n}\tilde{\Theta}_n\dot{\hat{\Theta}}_n. \tag{43}$$

From (6), one obtains

$$\varrho_n^{P_n-1} K(v) \leq \frac{\varrho_n^{2P_n-2}}{4} + \bar{K}^2. \tag{44}$$

Then we have

$$\begin{aligned}\mathscr{L}V_n \leq & -\sum_{j=1}^{n-1}\left(\frac{c_j \mathscr{B}_j}{P_j}\varrho_j^{p+1} - \frac{\gamma_j \tilde{\Theta}_j \hat{\Theta}_j}{r_j} - d_j\right) + \varrho_n^{P_n-1}\bar{f}_n(\boldsymbol{\mathcal{X}}_n) + \varrho_n^{P_n-1} k_0^{p_n} v^{p_n} + \bar{K}^2 \\ & - \frac{P_n-1}{P_n}\varrho_n^{P_n} + \frac{P_n-1}{4} - \frac{1}{r_n}\tilde{\Theta}_n \dot{\hat{\Theta}}_n \end{aligned} \tag{45}$$

where $\bar{f}_n(\boldsymbol{\mathcal{X}}_n) = (P_n-1)\varrho_n^{P_n-3}\|\boldsymbol{H}_n\|^4/4 + F_n(\bar{\boldsymbol{x}}_n) + \left[(p_{n-1}+1)\varrho_n^{p_n}\right]/(p+3) + (P_n-1)\varrho_n/P_n + \varrho_n^{P_n-1}/4$.

Given that Lemma 2–3, one obtains

$$\varrho_n^{P_n-1}\bar{f}_n(\boldsymbol{\mathcal{X}}_n) \leq \varrho_n^{p+3}\Phi_n + \frac{|\varrho_n|^{P_n-1}\tilde{\Theta}_n||\boldsymbol{\Psi}_n(\boldsymbol{\mathcal{X}}_n)||^2}{4a_n} + \frac{P_n-1}{P_n}\varrho_n^{P_n} + \frac{\epsilon_n^{P_n}}{P_n} + \varepsilon_n \tag{46}$$

where $\varepsilon_n, a_n \in \boldsymbol{R}^+$, and $\Phi_n = \left[\left((P_n-1)\psi_n\right)/(p+3)\right]^{(p+3)/(P_n-1)}\left[p_n/(P_n-1)\varepsilon_n\right]^{p_n/(P_n-1)}$, $\psi_n = \sqrt{1+\hat{\Theta}_n^2}||\boldsymbol{\Psi}_n(\boldsymbol{\mathcal{X}}_n)||^2/4a_n + a_n$.

Design v and $\dot{\hat{\Theta}}_n$ as

$$v \triangleq -\Omega_n \varrho_n, \tag{47}$$

$$\Omega_n = \left(\frac{\mathscr{B}_n}{P_n}c_n + \Phi_n\right)^{\frac{1}{p_n}}, \tag{48}$$

$$\dot{\hat{\Theta}}_n = \frac{r_n|\varrho_n|^{P_n-1}||\boldsymbol{\Psi}_n(\boldsymbol{\mathcal{X}}_n)||^2}{4a_n} - \gamma_n\hat{\Theta}_n \tag{49}$$

where $\hat{\Theta}_n(0) > 0$, $c_n, \gamma_n \in \boldsymbol{R}^+$, $\mathscr{B}_n = P_n/(p+3)$.

Substituting (44)-(49) to (43), and combining $-\varrho_j^{p+3} \leq \left(-\varrho_j^{P_j} + (p_j-1)/(p+3)\right)/\mathscr{B}_j$, one obtains

$$\mathscr{L}V_n \leq -\sum_{j=1}^{n}\left(\frac{c_j}{P_j}\varrho_j^{P_j} - \frac{\gamma_j\tilde{\Theta}_j\hat{\Theta}_j}{r_j} - \bar{d}_j\right) + \bar{K}^2 \tag{50}$$

where $\bar{d}_j = d_j + c_j(p_j-1)/P_j(p+3)$.

According to $\tilde{\Theta}_j\hat{\Theta}_j \leq -\tilde{\Theta}_j^2/2 + \Theta_j^2/2$, one obtains

$$\mathscr{L}V_n \leq -\sum_{j=1}^{n}\frac{c_j}{P_j}\varrho_j^{P_j} - \sum_{j=1}^{n}\frac{\gamma_j\tilde{\Theta}_j^2}{2r_j} + d \tag{51}$$

where $d = \sum_{j=1}^{n}\left(\bar{d}_j + \gamma_j\Theta_j^2/2r_j\right) + \bar{K}^2$.

3.3. Stability analysis

Theorem 1. *For IS-SHONS (1) with $e_1(0) \in \left(\underline{\mathcal{G}}(0), \bar{\mathcal{G}}(0)\right)$, the designed DFPPB-based fuzzy control algorithm guarantees that*

1) *All closed-loop signals remain SGBIP;*
2) *the system output is capable of effectively tracking the desired signal, while the tracking error e_1 is consistently kept within the DFPPB.*

Proof.

1) Let $V = V_n$, $c = \min_{1\leq j\leq n}\{c_j, 2\gamma_j\}$, we obtain from (51) that

$$\mathscr{L}V \leq -cV + d. \tag{52}$$

Given that (52) and Lemma 1, one obtains

$$\mathbb{E}(V) \leq V(0)\exp(-ct) + \frac{d}{c}. \tag{62}$$

Since $0 < \exp(-ct) \leq 1$, then

$$\mathbb{E}(V) \leq V(0) + \frac{d}{c} \tag{53}$$

meaning that V is SGBIP.

Given that the expression of V, one obtains

$$\mathbb{E}(|\varrho_i|) \leq \left[P_i\left(V(0) + \frac{d}{c}\right)\right]^{\frac{1}{P_i}}, \tag{54}$$

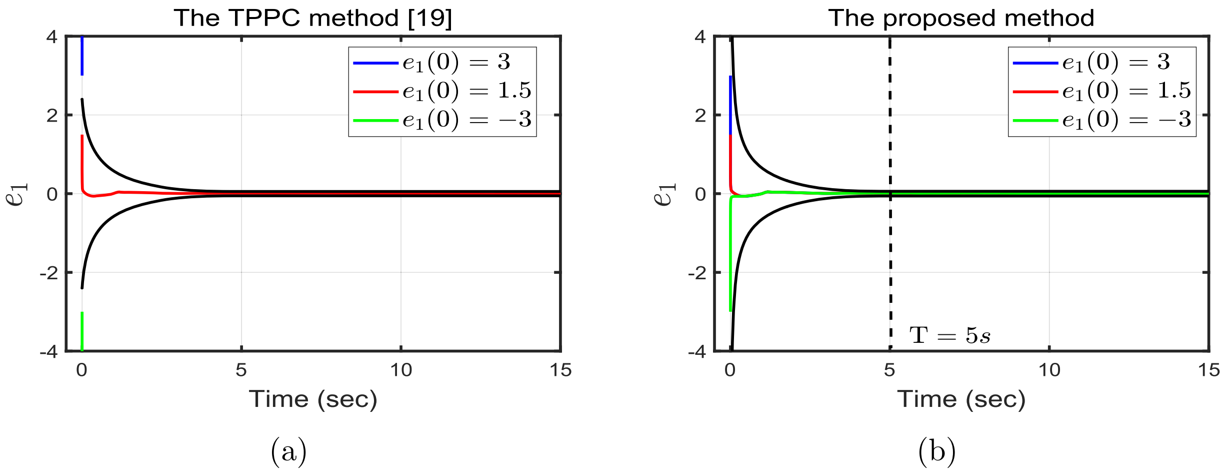

Fig. 10. (a)(b) represent the tracking error curves under the action of TPPC method [19] and the proposed method under three cases, respectively.

$$\mathbb{E}\left(|\tilde{\Theta}_i|\right) \le \sqrt{2r_i\left(V(0)+\frac{d}{c}\right)}. \tag{55}$$

From (54)-(55), it can be derived that $\tilde{\Theta}_i$ and ϱ_i are SGBIP. According to (30)-(32),(38)-(40) and (47)-(49), one can further derived that α_i, v and $\hat{\Theta}_i$ are SGBIP, then x_i is also SGBIP. In conclusion, all closed-loop signals are SGBIP.

2) According to (18), one know that $e_1(0) \in \left(\underline{\mathcal{G}}(0), \mathcal{G}(0)\right)$ is equivalent to $e_1(0) \in \left(\mathscr{H}\left(-\vartheta_1\Gamma(0)\right), \mathscr{H}\left(\vartheta_2\Gamma(0)\right)\right)$. Based on (18)-(22) and the boundedness of s, one know that $e_1(t) \in \left(\mathscr{H}\left(-\vartheta_1\Gamma(t)\right)/M(\sigma), \mathscr{H}\left(\vartheta_2\Gamma(t)/M(\sigma)\right)\right)$ holds for $\forall t \in \boldsymbol{R}^+$, i.e., $e_1(t) \in \left(\underline{\mathcal{G}}(t), \bar{\mathcal{G}}(t)\right)$ holds for $\forall t \in \boldsymbol{R}^+$. Based on the properties of $\mathscr{H}(\cdot)$ and $\Gamma(t)$, we can further derive that $e_1(t) \in \left(\mathscr{H}\left(-\vartheta_1\Gamma_{\mathrm{T}}\right)/M(\sigma), \mathscr{H}\left(\vartheta_2\Gamma_{\mathrm{T}}/M(\sigma)\right)\right)$ for $\forall t \geq \mathrm{T}$, where $\mathscr{H}\left(-\vartheta_1\Gamma_{\mathrm{T}}\right)$ and $\mathscr{H}\left(\vartheta_2\Gamma_{\mathrm{T}}\right)$ are constants. The aforementioned content indicates that the system output can track the desired signal, while $e_1(t)$ consistently remains within the DFPPB. □

Remark 4. It should be pointed out that in order to achieve "dual flexibility", the proposed control algorithm involves some parameters. The selection of parameters usually follows the following rules: 1)The design rules of $\Gamma_0, \mathrm{T}, \Gamma_{\mathrm{T}}, \ell$ are similar to the conventional UPPC method (see [38] for details); 2) τ is to control the expansion of the constrained boundary when input saturation occurs, and the larger the τ, the smaller the expansion. Of course, the pursuit of extreme performance also increases the complexity of algorithm design and calculation to a certain extent. In addition, the proposed algorithm only takes input saturation into account, but does not consider the global optimality under actuator faults [54,55], which will be an important direction for future efforts.

Remark 5. Note that the proposed method is indeed applicable to the situation where the initial error information is completely unknown, it seems that this situation is similar to being global boundedness. It should be noted that, on the one hand, the proposed method is a unified control algorithm applicable to various types, and when the error information is partially known and fully known, it is required that the initial error must be included within the initial boundary; on the other hand, this paper employs FLS to approximate the uncertain nonlinear function, based on the approximation rule of FLS, it can only approximate the uncertain nonlinear function within a bounded compact set. Therefore, based on the above analysis, the proposed method can only ensure that the closed-loop signal remain SGBIP.

4. Simulation

Example 1. Consider a IS-SHONS as follows

$$\begin{cases} \mathrm{d}x_1 = x_2^3\mathrm{d}t + \left(1-\cos x_1\right)\mathrm{d}w \\ \mathrm{d}x_2 = \left(-0.4x_1^2 - 0.4x_2^2\cos x_2 + \mathrm{S}^3(v)\right)\mathrm{d}t + \left(x_1\sin x_2\right)\mathrm{d}w \\ y_1 = x_1. \end{cases} \tag{56}$$

Obviously, the exponent of x_2 of the first sub-expression and the exponent of $S(v)$ of the second sub-expression are both 3, which is fundamentally different from the exponent of 1 in traditional feedback systems. Let $y_d = \sin(0.5t)$, $\mathrm{T}=5, \Gamma_{\mathrm{T}}=0.06, \ell=1, \tau=0.2$, $\rho_1=5, \rho_2=0.5, \bar{v}=2, c_i=40, \gamma_i=3, r_i=0.1, a_i=10$ with $i=1,2$, $\left[\hat{\Theta}_1(0), \hat{\Theta}_2(0)\right]^{\mathrm{T}} = [3,4]^{\mathrm{T}}$. Choose the fuzzy membership functions as: $\Psi_i = e^{-(Z_i-5+j)^2/2}, i=1,2, j=1,\cdots,9$. Let $\Gamma_0=\vartheta_i=1$, based on Remark 2, on know that the initial PPB is infinite, i.e., $\underline{\mathcal{G}}(0) \to -\infty$ and $\bar{\mathcal{G}}(0) \to +\infty$, which indicates that the proposed algorithm is applicable for the case where the initial error is entirely unknown. To validate this, two initial errors were selected: Case 1 with $e_1(0)=2$, Case 2 with $e_1(0)=-2$. The corresponding tracking performances,

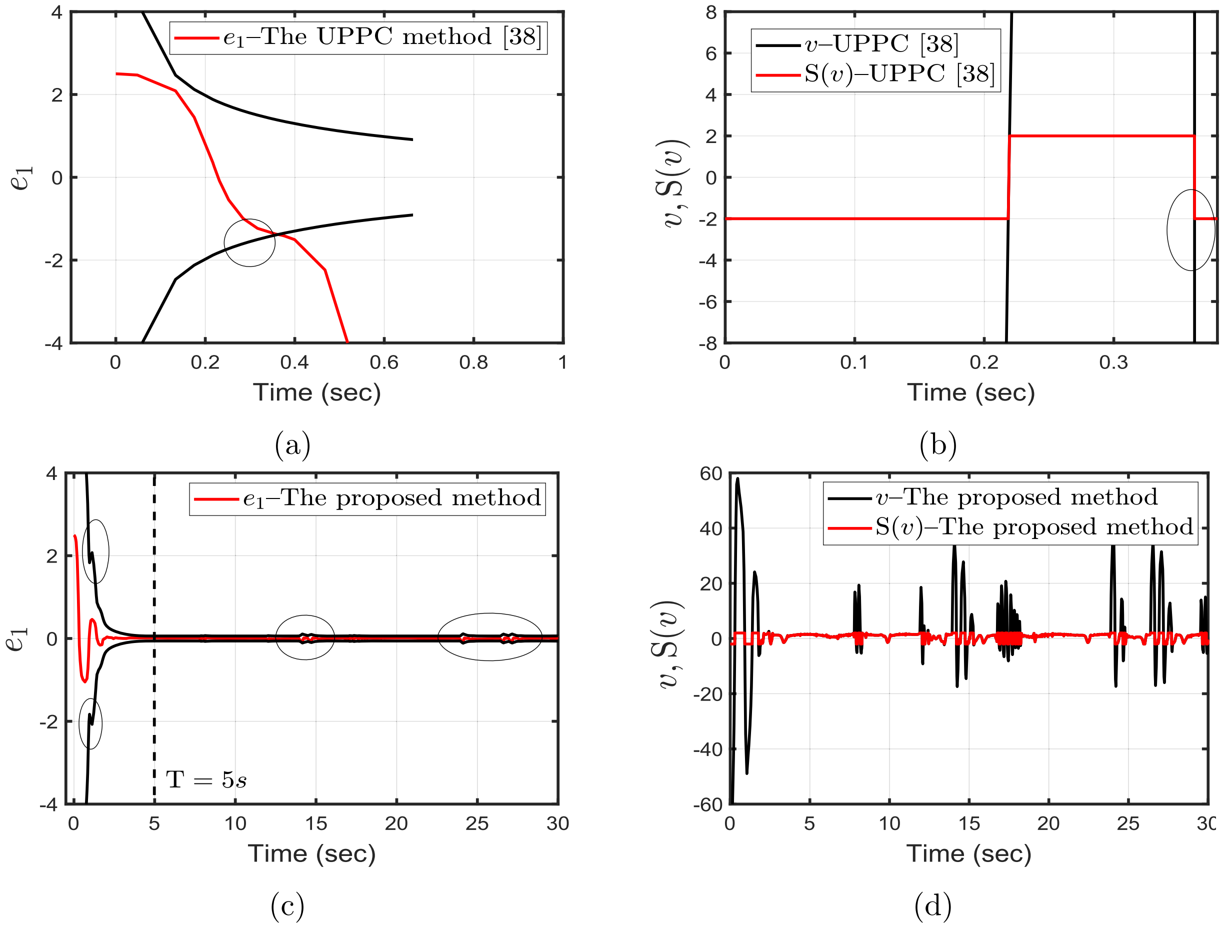

Fig. 11. (a)(b) respectively represent the tracking error curve and control input curve under the action of the UPPC method [38]; (c)(d) respectively represent the tracking error curve and control input curve under the action of the proposed method.

tracking errors, and control inputs for both cases are illustrated in Fig. 2 and Fig. 3, respectively. The results validate that the proposed method ensures that the system output is capable of effectively tracking the desired signal, while the tracking error $e_1(t)$ is consistently within the DFPPB.

To verify the flexibility of the proposed method, three different sets of parameters were selected: Case 1: $e_1(0) = 1.5, \vartheta_1 = 0.5, \Gamma_0 = \vartheta_2 = 1$, Case 2: $e_1(0) = -1.5, \vartheta_2 = 0.5, \Gamma_0 = \vartheta_1 = 1$, Case 3: $e_1(0) = 0.5, \vartheta_1 = \vartheta_2 = 0.5, \Gamma_0 = 0.9$. The tracking curves for all three cases are shown in Subgraph (a) of Fig. 4, with their individual responses depicted in Subgraphs (b)(c)(d) of Fig. 4. The results demonstrate that the proposed method can accommodate various cases through appropriate parameter adjustment.

To demonstrate the superiority of the proposed method, the comparison is conducted with the TPPC method [19] without considering the input saturation, i.e., $S(v) \equiv v$. Subgraphs (a) and (b) in Fig. 5 illustrate the tracking error curves of the TPPC and the proposed methods, respectively. It is evident that the TPPC method requires the initial PPB to be bounded, consequently, it is only applicable when the initial error falls within the PPB (e.g., $e_1(0) = 1.5$). However, for cases where the initial error exceeds the boundaries (e.g., $e_1(0) = 3$ and $e_1(0) = -3$), the TPPC method becomes inapplicable. In contrast, the proposed algorithm demonstrates the capability to effectively handle all three different initial error scenarios.

In addition, the comparison is conducted between the proposed method and the UPPC method [38]. Although the UPPC method can accommodate different initial error cases through parameter adjustment, it fails to address the prevalent input saturation issue in practical systems. As shown in Subgraphs (a) and (b) of Fig. 5, when the control input exceeds the saturation threshold, the tracking performance will diminish and even violate the PPB, and resulting in simulation failure. In contrast, this paper innovatively establishes an intrinsic connection between performance constraints and input saturation (see Remark 3 for details), enabling adaptive adjustment of PPB. Specifically, Subgraphs (c) and (d) of Fig. 5 demonstrate that the DFPPB adaptively expands when $|v| > \bar{v}$ to mitigate the impact of input saturation on tracking performance, while the DFPPB can adaptively revert to the original PPB when $|v| \le \bar{v}$. Consequently, the proposed algorithm achieves autonomous coordination between performance preset and input security (Fig. 6).

Remark 6. It is worth noting that some DPPC methods [35–37,55] utilizing shifting transformation and finite-time constraining function can also achieve the pre-set tracking performance without the conservative initial limitations, however, the limitation of

DPPC methods is also obvious, i.e., whether the initial error information is known, partially unknown or completely unknown, its initial PPB must always be infinite, when the error information is known or partially unknown, it will inevitably lead to the decline of the initial transient performance. Compared with them, the advantages of the proposed method are that it can not only be used in many cases where the initial error information is completely known, partially known and completely unknown without changing the control structure, but also achieve autonomous coordination between performance preset and input security.

Example 2. A simplified boiler unit model [9] is considered as follows

$$\begin{cases} \dot{x}_1 = x_2^3 \\ \dot{x}_2 = \frac{x_1^2}{1+x_2^2} + \mathrm{S}(v) \\ y = x_1, \end{cases} \tag{57}$$

where v denotes the control valve position, x_1 denotes the drum pressure, x_2 denotes the reheater pressure. The simplified boiler unit model is clearly a typical example of the high-order system. Let $y_d = \sin(0.5t) + 0.5\sin t$, $\mathrm{T} = 5, \Gamma_{\mathrm{T}} = 0.06, \ell = 1, \tau = 0.2, \rho_1 = 5, \rho_2 = 0.5, \bar{v} = 5, c_i = 40, \gamma_i = 3, r_i = 0.1, a_i = 10$ with $i = 1, 2$, $\left[\hat{\Theta}_1(0), \hat{\Theta}_2(0)\right]^{\mathrm{T}} = [3, 4]^{\mathrm{T}}$. Choose the fuzzy membership functions as: $\Psi_i = e^{-(Z_i-5+j)^2/2}, i = 1, 2, j = 1, \cdots, 9$. Let $\Gamma_0 = \vartheta_i = 1$, and select two initial errors: Case 1: $e_1(0) = 2$, Case 2: $e_1(0) = -2$. The tracking curves, tracking error curves, and control input curves for the two cases are respectively given in Fig. 7 and Fig. 8. It means that the system output is capable of tracking the desired signal, and the tracking error e_1 is consistently retained within the DFPPB.

To verify the flexibility of the proposed method, three different sets of parameters were selected: Case 1: $e_1(0) = 1.5, \vartheta_1 = 0.5, \Gamma_0 = \vartheta_2 = 1$, Case 2: $e_1(0) = -1.5, \vartheta_2 = 0.5, \Gamma_0 = \vartheta_1 = 1$, Case 3: $e_1(0) = 0.5, \vartheta_1 = \vartheta_2 = 0.5, \Gamma_0 = 0.9$. The tracking curves for all three cases are shown in Subgraph (a) of Fig. 9, with their individual responses depicted in Subgraphs (b)(c)(d) of Fig. 9. The results demonstrate that the proposed method can accommodate various cases through appropriate parameter adjustment.

The comparison is conducted with the TPPC method [19] without considering the input saturation, i.e., $\mathrm{S}(v) \equiv v$. Subgraphs (a) and (b) in Fig. 10 illustrate the tracking error curves of the TPPC and the proposed methods, respectively. As shown in subgraph (a) of Fig. 10, the TPPC method is solely suitable for initial errors confined within the PPB (like $e_1(0) = 1.5$), but not for cases with $e_1(0) = 3$ and $e_1(0) = -3$. Conversely, the proposed algorithm is well-suited for the three different initial errors.

The comparison is also conducted between the proposed method and the UPPC method [38]. As shown in Subgraph (a)(b) of Fig. 11, when the control input exceeds the saturation threshold, the tracking performance will diminish and even violate the PPB, resulting in simulation failure. However, From subgraph (c)(d) of Fig. 11, one know that the DFPPB adaptively expands when $|v| > \bar{v}$ to mitigate the impact of input saturation on tracking performance, while the DFPPB can adaptively revert to the original PPB when $|v| \leq \bar{v}$.

5. Conclusion

A DFPPB-based fuzzy control approach for IS-SHONSs is first present in this article. By designing a RF-based PPB, the proposed algorithm be used in many cases where the initial error information is completely known, partially known and completely unknown without changing the control structure. In addition, by designing an auxiliary system and embedding its output into PPB, and a novel DFPPB and a tensile model-based barrier function are constructed, so that the proposed algorithm achieves autonomous coordination between performance preset and input security. It is worth noting that the proposed algorithm does not take into account global optimality and actuator faults [54,55], the future research will primarily concentrate on the DFPPB-based reinforcement learning control and fault-tolerant control for IS-SHONSs.

CRediT authorship contribution statement

Ziyi Liu: Writing – original draft; **Yangang Yao:** Writing – original draft; **Yu Kang:** Writing – review & editing; **Yunbo Zhao:** Writing – review & editing; **Jieqing Tan:** Writing – review & editing; **Lichuan Gu:** Writing – review & editing; **Qiang Li:** Writing – review & editing.

Declaration of competing interest

The authors declare that they have no known competing financial interests or personal relationships that could have appeared to influence the work reported in this paper.

Acknowledgments

This work was supported in part by the Natural Science Foundation of Anhui Province under Grant (2508085MF165 and 2408085QA008), Anhui Provincial Department of Education Research Project under Grant 2024AH040082, the Open Fund of State Key Laboratory of Tea Plant Biology and Utilization under grant SKLTOF20240112, and also supported in part by the National Natural Science Foundation of China (62033012, 62103394, 62173317, 61725304, 32472007 and 62406005).

References

[1] W. Li, M. Krstic, Mean-nonovershooting control of stochastic nonlinear systems, IEEE Trans. Autom. Control. 66 (12) (2020) 5756–5771.
[2] Y. Zhang, L. Xie, X. Xie, Z. Sun, K. Zhang, Fuzzy adaptive control for stochastic nonstrict feedback systems with multiple time-delays: a novel lyapunov-krasovskii method, IEEE Trans. Fuzzy Syst. 32 (6) (2024) 3815–3824.
[3] Y.G. Yao, J.Q. Tan, J. Wu, X. Zhang, Event-triggered fixed-time adaptive fuzzy control for state-constrained stochastic nonlinear systems without feasibility conditions, Nonlinear Dyn. 105 (2021) 403–416.
[4] Y.G. Yao, J.Q. Tan, J. Wu, X. Zhang, Event-triggered fixed-time adaptive neural dynamic surface control for stochastic non-triangular structure nonlinear systems, Inf. Sci. 569 (2021) 527–543.
[5] Y.G. Yao, J.Q. Tan, J. Wu, X. Zhang, Decentralized fixed-time control for state-constrained stochastic systems via nonlinear state-dependent function approach, Int. J. Robust. Nonlinear Control. 32 (8) (2022) 4923–4945.
[6] X. Xie, N. Duan, Output tracking of high-order stochastic nonlinear systems with application to benchmark mechanical system, IEEE Trans. Autom. Control. 55 (5) (2010) 1197–1202.
[7] G. Li, X. Xie, Adaptive state-feedback stabilization of stochastic high-order nonlinear systems with time-varying powers and stochastic inverse dynamics, IEEE Trans. Autom. Control. 65 (12) (2020) 5360–5367.
[8] H. Min, S. Xu, J. Gu, B. Zhang, Z. Zhang, Further results on adaptive stabilization of high-order stochastic nonlinear systems subject to uncertainties, IEEE Trans. Neural Netw. Learn. Syst. 31 (1) (2020) 225–234.
[9] F. Fang, L. Ma, S. Ding, J. Park, Finite-time stabilization of high-order stochastic nonlinear systems with asymmetric output constraints, IEEE Trans. Syst. Man Cybern. Syst. 51 (11) (2021) 7201–7213.
[10] S. Liu, B. Niu, G. Zong, X. Zhao, N. Xu, Adaptive neural dynamic-memory event-triggered control of high-order random nonlinear systems with deferred output constraints, IEEE Trans. Autom. Sci. Eng. 21 (3) (2024) 2779–2791.
[11] Y.G. Yao, J.Q. Tan, J. Wu, X. Zhang, A unified fuzzy control approach for stochastic high-order nonlinear systems with or without state constraints, IEEE Trans. Fuzzy Syst. 30 (10) (2022) 4530–4540.
[12] A. Polyakov, D. Efimov, W. Perruquetti, Finite-time and fixed-time stabilization: implicit lyapunov function approach, Automatica 51 (2015) 332–340.
[13] M. Jiang, X. Xie, K. Zhang, Finite-time stabilization of stochastic high-order nonlinear systems with FT-SISS inverse dynamic, IEEE Trans. Autom. Control. 64 (1) (2019) 313–320.
[14] W. Li, M. Krstic, Prescribed-time output-feedback control of stochastic nonlinear systems, IEEE Trans. Autom. Control. 68 (3) (2023) 1431–1446.
[15] Y.G. Yao, Y. Kang, Y. Zhao, P. Li, J.Q. Tan, A novel prescribed-time control approach of state-constrained high-order nonlinear systems, IEEE Trans. Syst. Man Cybern. Syst. 54 (5) (2024) 2941–2951.
[16] Y.G. Yao, K. Kang, Y. Zhao, P. Li, J.Q. Tan, Prescribed-time output feedback control for cyber-physical systems under output constraints and malicious attacks, IEEE Trans. Cybern. 54 (11) (2024) 4530–4540.
[17] L. Zhang, X. Liu, C. Hua, Prescribed-time control for stochastic high-order nonlinear systems with parameter uncertainty, IEEE Trans. Circuits Syst. II Exp. Briefs 70 (11) (2023) 4083–4087.
[18] Y.G. Yao, Y. Kang, Y. Zhao, P. Li, J.Q. Tan, Unified fuzzy control of high-order nonlinear systems with multi-type state constraints, IEEE Trans. Cybern. 54 (4) (2024) 2525–2535.
[19] C. Bechlioulis, G. Rovithakis, Robust adaptive control of feedback linearizable MIMO nonlinear systems with prescribed performance, IEEE Trans. Autom. Control/. 53 (9) (2008) 2090–2099.
[20] W. Sun, S. Su, Y. Wu, J. Xia, Adaptive fuzzy event-triggered control for high-order nonlinear systems with prescribed performance, IEEE Trans. Cybern. 52 (5) (2022) 2885–2895.
[21] Y. Liu, H. Ma, Adaptive fuzzy tracking control of nonlinear switched stochastic systems with prescribed performance and unknown control directions, IEEE Trans. Syst. Man. Cybern. Syst. 50 (2) (2020) 590–599.
[22] C. Hua, L. Zhang, X. Guan, Decentralized output feedback adaptive NN tracking control for time-delay stochastic nonlinear systems with prescribed performance, IEEE Trans. Neural Netw. Learn. Syst. 26 (11) (2015) 2749–2759.
[23] W. Si, D. Dong, F. Yang, Decentralized adaptive neural prescribed performance control for high-order stochastic switched nonlinear interconnected systems with unknown system dynamics, ISA Trans. 84 (2019) 55–68.
[24] Q. Zhou, H. Li, L. Wang, R. Lu, Prescribed performance observer-based adaptive fuzzy control for nonstrict-feedback stochastic nonlinear systems, IEEE Trans. Syst. Man Cybern. Syst. 48 (10) (2018) 1747–1758.
[25] S. Sui, C. Chen, S. Tong, Finite-time adaptive fuzzy prescribed performance control for high-order stochastic nonlinear systems, IEEE Trans. Fuzzy Syst. 30 (7) (2022) 2227–2240.
[26] B. Xin, S. Cheng, Q. Wang, J. Chen, F. Deng, Fixed-time prescribed performance consensus control for multiagent systems with nonaffine faults, IEEE Trans. Fuzzy Syst. 31 (10) (2023) 3433–3446.
[27] Z. Liang, Z. Wang, J. Zhao, P.K. Wong, Z. Yang, Z. Ding, Fixed time and fault-tolerant path-following control for autonomous vehicles with unknown parameters subject to prescribed performance, IEEE Trans. Syst. Man Cybern. Syst. 53 (4) (2023) 2363–2373.
[28] H. Duan, Y. Yuan, Z. Zeng, Distributed robust learning control for multiple unmanned surface vessels with fixed-time prescribed performance, IEEE Trans. Syst. Man Cybern. Syst. 54 (2) (2024) 787–799.
[29] K. Zhao, Y. Song, T. Ma, L. He, Prescribed performance control of uncertain euler-Lagrange systems subject to full-state constraints, IEEE Trans. Neural Netw. Learn. Syst. 29 (8) (2018) 3478–3489.
[30] K. Zhao, Y. Song, Y. Wang, Regular error feedback based adaptive practical prescribed time tracking control of normal-form nonaffine systems, J. Franklin Inst. 356 (5) (2019) 2759–2779.
[31] K. Sun, R. Guo, J. Qiu, Fuzzy adaptive switching control for stochastic systems with finite-time prescribed performance, IEEE Trans. Cybern. 52 (9) (2022) 9922–9930.
[32] Y.G. Yao, J.Q. Tan, J. Wu, X. Zhang, Event-triggered finite-time adaptive fuzzy tracking control for stochastic nontriangular structure nonlinear systems, Int. J. Fuzzy Syst. 23 (2021) 2157–2169.
[33] J.X. Zhang, T. Chai, Proportional-integral funnel control of unknown lower-triangular nonlinear systems, IEEE Trans. Autom. Control. 69 (3) (2024) 1921–1927.
[34] Y. Liu, X. Liu, Y. Jing, X. Chen, J. Qiu, Direct adaptive preassigned finite-time control with time-delay and quantized input using neural network, IEEE Trans. Neural Netw. Learn. Syst. 31 (4) (2020) 1222–1231.
[35] J.X. Zhang, Q.G. Wang, W. Ding, Global output-feedback prescribed performance control of nonlinear systems with unknown virtual control coefficients, IEEE Trans. Autom. Control. 67 (12) (2022) 6904–6911.
[36] G.P. Liu, Y. Zhang, C.C. Hua, Li y f, chen j n. adaptive fuzzy tracking control for nonlinear time-delay systems with performance constrained by deferred monotone tube boundaries, IEEE Trans. Fuzzy Syst. 32 (11) (2024) 6136–6148.
[37] Z.Y. Gao, Z.C. Sun, G. Guo, Adaptive predefined-time tracking control for vehicular platoons with finite-time global prescribed performance independent of initial conditions, IEEE Trans. Veh. Technol. 73 (11) (2024) 16254–16267.
[38] K. Zhao, F. Lewis, L. Zhao, Unifying performance specifications in tracking control of MIMO nonlinear systems with actuation faults, Automatica 155 (2023) 111102.
[39] L. Li, K. Zhao, Z. Zhang, Y. Song, Dual-channel event-triggered robust adaptive control of strict-feedback system with flexible prescribed performance, IEEE Trans. Autom. Control. 69 (3) (2024) 1752–1759.
[40] Z. Li, Y. Wang, Y. Song, Asymptotic tracking control of SISO nonlinear systems with unknown time-varying coefficients: a global performance guaranteed solution, IEEE Trans. Syst. Man Cybern. Syst. 54 (6) (2024) 3717–3727.

[41] L. Li, K. Zhao, Y. Song, F L. Lewis, On the uniformness of full-state error prescribed performance for strict-feedback systems, IEEE Trans. Syst. Man Cybern. Syst. 54 (5) (2024) 3022–3031.
[42] Q. Bai, K. Zhao, Y. Song, Unified adaptive performance control of MIMO input-quantized nonlinear systems, IEEE Trans. Circuit. Syst. I Regular Papers 71 (7) (2024) 3331–3342.
[43] Y. Yang, J. Tan, D. Yue, Prescribed performance tracking control of a class of uncertain pure-feedback nonlinear systems with input saturation, IEEE Trans. Syst. Man Cybern. Syst. 50 (5) (2020) 1733–1745.
[44] Y. Sun, J. Liu, Y. Gao, Z. Liu, Y. Zhao, Adaptive neural tracking control for manipulators with prescribed performance under input saturation, IEEE/ASME Trans. Mechatron. 28 (2) (2023) 1037–1046.
[45] H. Shen, X. Yu, H. Yan, J.H. Park, J. Wang, Robust fixed time sliding mode attitude control for a 2-DOF helicopter subject to input saturation and prescribed performance, IEEE Trans. Transport. Electrific. 11 (1) (2024).
[46] K. Yong, M. Chen, Y. Shi, Q. Wu, Flexible performance-based robust control for a class of nonlinear systems with input saturation, Automatica 122 (2020) 109268.
[47] Y.G. Yao, Y. Kang, Y.B. Zhao, P.F. Li, J.Q. Tan, Flexible prescribed performance output feedback control for nonlinear systems with input saturation, IEEE Trans. Fuzzy Syst. 32 (11) (2024) 6012–6022.
[48] X. Yue, H. Zhang, J. Sun, L. Wan, Adaptive event-triggered saturation-tolerant control for multi-agent systems based on finite time fuzzy learning, IEEE Trans. Fuzzy Syst. 32 (10) (2024) 5638–5647.
[49] H. Xie, G. Zong, D. Yang, X. Zhao, Y. Yi, Flexible-fixed-time performance-based adaptive asymptotic tracking control of switched nonlinear systems with input saturation, IEEE Trans. Autom. Sci. Eng. 21 (4) (2024).
[50] Y.G. Yao, Y. Kang, Y. Zhao, J. Tan, L. Gu, G. Shi, Sliding flexible prescribed performance control for input saturated nonlinear systems, IEEE Trans. Fuzzy Syst. 33 (4) (2025) 1241–1252.
[51] R. Ji, D. Li, S.S. Ge, Saturation-tolerant prescribed control for nonlinear time-delay systems, IEEE Trans. Fuzzy Syst. 31 (8) (2023) 2495–2508.
[52] Y.G. Yao, Z.Y. Liu, Y. Kang, Y. Zhao, J. Tan, L. Gu, Q. Li, J.L. Wang, Sliding flexible prescribed performance boundary-guided reinforcement learning control for input-constrained nonlinear systems, IEEE Trans. Cybern. (2025). https://doi.org/10.1109/TCYB.2025.3610913
[53] Y.G. Yao, X. Liang, Y. Kang, Y. Zhao, J.Q. Tan, L. Gu, Dual flexible prescribed performance control of input saturated high-order nonlinear systems, IEEE Trans. Cybern. 55 (3) (2025) 1147–1158.
[54] S. Yu, H. Zhang, J. Sun, J. Zhang, Reinforcement learning-based fault-tolerant control for output-constrained nonlinear systems with preassigned-time performance, IEEE Trans. Circuit. Syst. I: Regular Papers 72 (10) (2025) 6097–6107.
[55] Q. Yang, H. Li, Z. Ruan, B. Fan, S.S. Ge, Reinforcement learning-based fault-tolerant control of uncertain strict-feedback nonlinear systems with intermittent actuator faults, IEEE Trans. Neural Netw. Learn. Syst. 36 (6) (2025) 10464–10478.